Neogene landscape evolution in the Andes of north-central Chile between 28 and 32°S: interplay between tectonic and erosional processes

MARÍA PÍA RODRÍGUEZ[1,2]*, GERMÁN AGUILAR[2], CONSTANZA URRESTY[1] & REYNALDO CHARRIER[1,3]

[1]*Departamento de Geología, Facultad de Ciencias Físicas y Matemáticas, Universidad de Chile, Santiago, Chile*

[2]*Advanced Mining Technology Center (AMTC), Facultad de Ciencias Físicas y Matemáticas, Universidad de Chile, Santiago, Chile*

[3]*Escuela de Ciencias de la Tierra, Universidad Andrés Bello, Campus República, Santiago, Chile*

**Corresponding author (e-mail: maria.p.rodriguez@gmail.com)*

Abstract: We combine geomorphological analysis of palaeosurfaces and U–Pb zircon geochronology of overlying tuffs to reconstruct the Neogene landscape evolution in north-central Chile (28–32°S). Prior to the Early Miocene, a pediplain dominated the landscape of the present-day Coastal Cordillera. The pediplain was offset during the Early (Middle?) Miocene, leading to uplift of the present-day eastern Coastal Cordillera and to the formation of a secondary topographic front. During the Late Miocene, the entire Coastal Cordillera was uplifted, with resulting deposition taking place within river valleys similar to those of the present day. A new pediplain developed on top of these deposits between the Early to Middle Pleistocene and was finally uplifted post-500 ka. These three major uplift stages correlate with episodes of increased deformation widely recognized throughout the Central Andes, starting after a Late Oligocene–Early Miocene episode of increased plate convergence. North of 30°S, the previous palaeotopography along the western Coastal Cordillera probably influenced Neogene landscape evolution. The presence of an inherited palaeotopography together with a strong decrease of precipitation to the north of 30°S would have determined differences in landscape development between this area and the area to the south of 30°S since the Early Miocene.

The morphology of active mountain belts results from the interplay between tectonic processes, which deform the lithosphere and result in uplifted regions of the Earth's surface, and erosional processes, which are mainly controlled by climate and rock type (Strecker *et al.* 2007). In the Central Andes (15–34°S, Fig. 1), along-strike variations of topography and the amount of shortening have been mostly related to north–south-changing tectonic features. The most widely mentioned correspond to subduction geometry (Jordan *et al.* 1983; Isacks 1988), the age of the Nazca Plate (Ramos *et al.* 2004) and interplate coupling (Lamb & Davis 2003). It is thought that these tectonic factors together with the pre-Neogene geological history (Ramos *et al.* 1996; Lamb *et al.* 1997; Tassara & Yañez 2003; Giambiagi *et al.* 2012) may have played a dominant role in the first-order topography and structure of the Andes (Hilley & Coutand 2010). However, it is also likely that erosional processes may influence the kinematics of deformation (Sobel & Strecker 2003; Hilley *et al.* 2004) and control the response time to uplift (Aguilar *et al.* 2011; Carretier *et al.* 2013) at the scale of morphostructural segments (Fig. 1; Hilley & Coutand 2010). Here, we present the case of the Central Andes of north-central Chile between 28° and 32°S, whose Neogene landscape evolution may have been influenced by several factors. Firstly, this region is located on the Pampean or Chilean flat-slab segment (27–33°S), within which the subduction angle between the Nazca and South American Plates is *c.* 10°, contrary to the adjacent regions of the Central Andes where this angle is *c.* 30° (Cahill & Isacks 1992). Slab flattening is thought to be related to the subduction of the buoyant Juan Fernández Ridge (Fig. 1), which migrated from the northern to the southern part of the study area between *c.* 16 and 12 Ma (Yañez *et al.* 2001). However, it is unclear if Neogene crustal thickening and uplift are a consequence of the subduction of the Juan Fernández Ridge (Cembrano *et al.* 2003) or are better related to changes in the convergence parameters between the Nazca

From: Sepúlveda, S. A., Giambiagi, L. B., Moreiras, S. M., Pinto, L., Tunik, M., Hoke, G. D. & Farías, M. (eds) 2015. *Geodynamic Processes in the Andes of Central Chile and Argentina*. Geological Society, London, Special Publications, **399**, 419–446. First published online April 4, 2014, http://dx.doi.org/10.1144/SP399.15

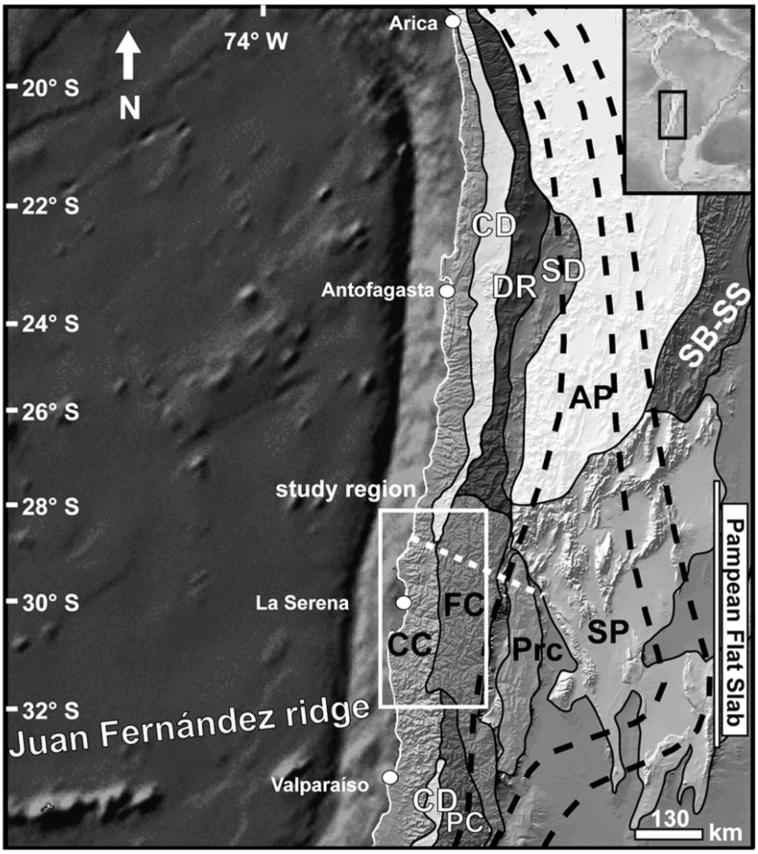

Fig. 1. Morphostructural units and tectonic setting of the Central Andes (15–34°S). Dashed black lines mark depth contour lines of the Nazca Plate underneath the South America Plate at 100, 150 and 200 km (Cahill & Isacks 1992). Dashed white line marks the symmetry axis of the Vallenar Orocline (Arriagada *et al.* 2009). CC, Coastal Cordillera; CD, Central Depression; DR, Domeyko Cordillera; SD, Subandean Depression; AP, Altiplano-Puna (including the Western and Eastern Cordilleras); SB, Subandean Ranges; SS, Santa Bárbara System; FC, Frontal Cordillera; Prc, Precordillera; SP, Sierras Pampeanas; PC, Principal Cordillera.

and South American Plates (Kay & Mpodozis 2002; Charrier *et al.* 2013).

Secondly, the study area also records a transition in the pre-Neogene topography that is reflected in the presence of the Vallenar Orocline at this latitude of the Central Andes (Fig. 1; Arriagada *et al.* 2009). The Vallenar Orocline is thought to mark the southernmost extent of Eocene–Oligocene deformation (Arriagada *et al.* 2009), associated with the so-called Incaic Range (Steinmann 1929; Charrier & Vicente 1972; Cornejo *et al.* 2003). During the Eocene and Oligocene the Incaic Range was the main palaeogeographic feature to the north of 31°S (Fig. 1; Maksaev & Zentilli 1999; Charrier *et al.* 2007; Arriagada *et al.* 2009, 2013; Bissig & Riquelme 2010), while an extensional volcano-sedimentary basin, known as the Abanico Basin (Charrier *et al.* 2002), developed south of 32°S. However, it is unclear how the presence of the Incaic relief may have influenced the subsequent landscape evolution throughout the studied area.

Thirdly, the region of north-central Chile has a semi-arid climate, which is transitional between the hyperarid conditions of the southern Atacama Desert north of 27°S and the more humid conditions of central Chile south of 33°S (Fig. 2a). The Southeast Pacific anticyclone (SEP) is the main factor responsible for the hyperaridity north of 27°S, whereas the penetration of the southern hemisphere westerlies results in the more humid conditions of central Chile (Veit 1996). In particular, along the studied region a north-to-south rise in precipitation occurs at 30°S related to the influence of the SEP (Fig. 2a). During the Palaeogene, the climate in north-central Chile was warmer and more humid than at present as indicated by the woody components of palaeoflora from fossiliferous localities just south of La Serena (Fig. 2a; Villagrán *et al.* 2004). Since *c.* 21 to 15 Ma subtropical vegetation has been replaced by sclerophytic shrubs indicating a warm, seasonal climate receiving scarce rainfall from both the east and the west (Villagrán *et al.* 2004). The transition between a hyperarid climate to the north of 27°S and a humid climate south of 33°S occurred after the Middle Miocene (Le Roux 2012). During this period the combination of a series of events, including glaciations in West Antartica, formation of the Humboldt Current and uplift of the Andes, are thought to have been responsible for the development of the latitudinal precipitation gradient throughout the study area (Le Roux 2012). The role, if any, that the present-day along-strike increase in precipitation and/or climatic changes throughout the Miocene could have played in shaping the landscape in north-central Chile is largely unknown.

In this study we combine geomorphological analysis of sub-planar palaeosurfaces in the Coastal Cordillera (Fig. 1) with the U–Pb zircon geochronology of overlying tuffs to reconstruct the Neogene history of uplift and incision of these palaeosurfaces in north-central Chile (28–32°S). Our results are discussed considering previous data on sub-planar palaeosurfaces in the Coastal Cordillera (Rodríguez *et al.* 2013) and the higher Frontal Cordillera (e.g. Bissig *et al.* 2002; Nalpas *et al.* 2009). Finally, we discuss the roles that tectonic and erosional processes have played in the development of the present-day topography in north-central Chile.

Regional framework

The large-scale geomorphology of the study area is characterized by a marked rise in mean elevation along west–east transects (Fig. 2b, d; Aguilar *et al.* 2011, 2013). This first-order geomorphological feature represents a topographic front separating two north–south-elongated morphostructural units corresponding to the Coastal Cordillera and Frontal Cordillera from west to east (Fig. 2b, c). Contrary to what is observed in the Andean segments to the north of 27°S and to the south of 33°S, no continuous Central Depression is observed to the east of the Coastal Cordillera in the study region (Figs 1 & 2c). Only north of 30°S is there an area which corresponds to that of relatively lower topography within the Coastal Cordillera (the Domeyko Depression; Fig. 2c).

The Coastal Cordillera is characterized to the west by a series of shore platforms displaying low slope values (<20°) (Fig. 2c; Paskoff 1970; Ota *et al.* 1995; Benado 2000; Saillard *et al.* 2009; Rodríguez *et al.* 2013). To the east, the Coastal Cordillera reaches a maximum elevation of *c.* 3200 m above mean sea-level (a.s.l.) (Fig. 2b). The Coastal Cordillera mainly corresponds to an east-dipping homoclinal block of Triassic–Lower Cretaceous volcano-sedimentary rocks that unconformably cover a Devonian–Carboniferous (Permian?) metamorphic and sedimentary basement (Fig. 3; Rivano & Sepúlveda 1991). Both features are intruded by Triassic–Early Cretaceous north–south-elongated plutonic belts with increasing ages to the east (Fig. 3; Rivano & Sepúlveda 1991; Emparán & Pineda 2006; Arévalo *et al.* 2009). Towards the border with the Frontal Cordillera, the Lower Cretaceous rocks at the top of the east-dipping homoclinal block are unconformably covered by subhorizontal Upper Cretaceous–Paleocene volcano-sedimentary rocks and intruded by a plutonic belt of similar age (Fig. 3; Pineda & Emparán 2006; Pineda & Calderón 2008). Along the coast and within the main valleys, Neogene marine and continental sedimentary rocks are exposed (Fig. 4; Rivano & Sepúlveda 1991; Le Roux *et al.* 2004, 2005, 2006; Emparán & Pineda 2006; Arévalo *et al.* 2009). As will be explained later, these deposits are closely related to the development of the pediplains studied here. The Coquimbo Formation corresponds to a shallow marine-to-transitional sedimentary succession exposed along the coast near the localities of Punta Choros and Tongoy (Figs 3 & 4). It records continuous marine deposition from the Early Miocene (*c.* 23 Ma) to the Early Pleistocene (*c.* 1 Ma) (Le Roux *et al.* 2004, 2005, 2006). South of 30°S, the Coquimbo Formation grades laterally towards the east into the continental Confluencia Formation (Figs 3 & 4). The Confluencia Formation is composed of fluvial and alluvial facies exposed along the lower and middle courses of the main valleys (Figs 3 & 4). The fluvial deposits change laterally towards the valley walls into the alluvial deposits (Fig. 4). In some areas the latter overlie the fluvial deposits (Fig. 4). No geochronological constraints exist for the Confluencia Formation, but based on its relationship with the Coquimbo Formation, a general Miocene–Pleistocene age can be assumed (Emparán & Pineda 2006). The alluvial facies within the Confluencia Formation present an interbedded ash bed south of Tongoy (Figs 3 & 4), which has been correlated with a similar level within the marine Coquimbo Formation exposed just to the west (Figs 3 & 4; Emparán & Pineda 2006) and dated at *c.* 6 Ma (Emparán & Pineda 2000). North of 30°S, the Domeyko Gravels are exposed within the Domeyko Depression (Figs 3 & 4). The Domeyko Gravels are alluvial deposits interpreted to have accumulated in a closed basin with a local sediment source (Arévalo *et al.* 2009).

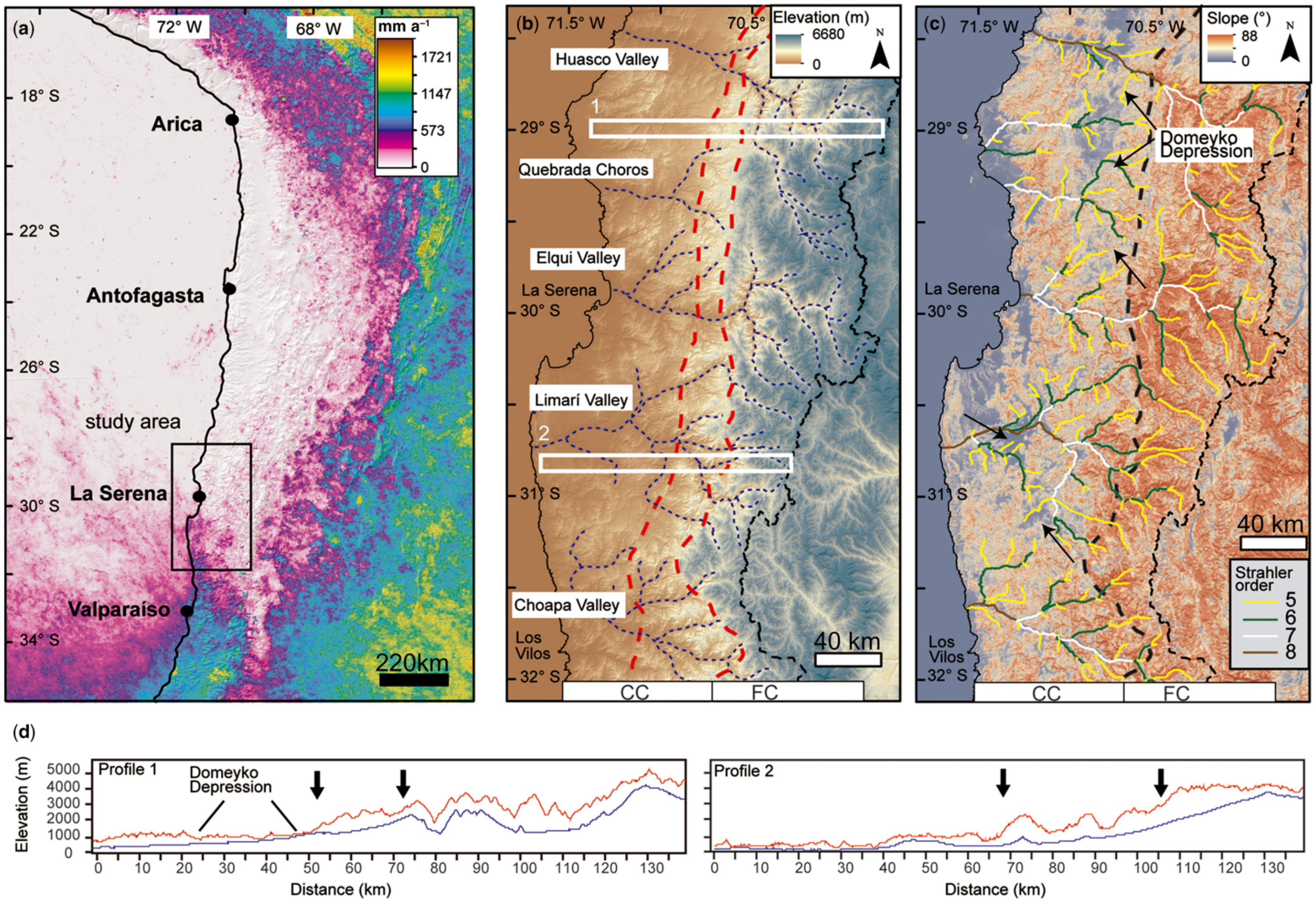
(a)
72° W
68° W
mm a⁻¹
1721
1147
573
0
18° S
Arica
22° S
Antofagasta
26° S
study area
La Serena
30° S
Valparaíso
34° S
220km
(b)
71.5° W
70.5°
Elevation (m)
6680
0
N
Huasco Valley
1
29° S
Quebrada Choros
Elqui Valley
La Serena
30° S
Limarí Valley
2
31° S
Choapa Valley
Los Vilos
32° S
40 km
CC
FC
(c)
71.5° W
70.5° W
Slope (°)
88
0
N
29° S
Domeyko Depression
La Serena
30° S
31° S
40 km
Strahler order
5
6
7
8
Los Vilos
32° S
CC
FC
(d)
Profile 1
Domeyko Depression
Elevation (m)
5000
4000
3000
2000
1000
0
0
10
20
30
40
50
60
70
80
90
100
110
120
130
Distance (km)
Profile 2
Distance (km)

There are no chronostratigraphic or geochronological constraints available for the Domeyko Gravels. However, they are thought to be of Middle Miocene age (Arévalo *et al.* 2009) according to regional correlations with the Atacama Gravels at *c.* 27°S (Mortimer 1973). Deposition of the Atacama Gravels started *c.* 17 Ma and ended by *c.* 10 Ma (Cornejo *et al.* 1993), finally leading to regional pedimentation and development of the Atacama Pediplain on top. Also exposed within the Domeyko Depression are alluvial and colluvial deposits that crop out attached to relatively higher topographic areas and that overlie the Domeyko Gravels (Fig. 4; Arévalo *et al.* 2009). No direct geochronological contraints are available for these deposits, but they have been correlated with similar deposits at 27°S (Arévalo *et al.* 2009) presenting intercalated ash units with ages between *c.* 7 and 3 Ma (Fig. 4; Arévalo *et al.* 2009). The alluvial and colluvial deposits exposed north of 30°S are correlated with the alluvial facies of the Confluencia Formation exposed south of 30°S.

The Frontal Cordillera reaches elevations as high as *c.* 6700 m a.s.l. It is formed by a core of Carboniferous to Permian magmatic units (Fig. 3; Nasi *et al.* 1990; Pineda & Calderón 2008), which here is referred to as the central Frontal Cordillera (Fig. 5). The core is covered to the west by a dominantly west-dipping block of Triassic–Upper Cretaceous folded volcano-sedimentary rocks, intruded by a Late Cretaceous–Early Paleocene magmatic belt (Mpodozis & Cornejo 1988; Nasi *et al.* 1990; Pineda & Emparán 2006; Pineda & Calderón 2008). This area will be referred to below as the western Frontal Cordillera (Fig. 5). To the east, the basement core is intruded by, or in faulted contact with, a block composed mostly of Permo-Triassic magmatic and volcanic rocks unconformably overlain by Oligocene–Miocene folded volcano-sedimentary rocks (Fig. 3; Maksaev *et al.* 1984; Nasi *et al.* 1990; Martin *et al.* 1999; Bissig *et al.* 2001; Winocur *et al.* 2014). These rocks are unconformably covered by Miocene subhorizontal volcanic rocks and intruded by a north–south-trending Oligocene magmatic belt (Fig. 3; Maksaev *et al.* 1984; Nasi *et al.* 1990; Martin *et al.* 1999; Bissig *et al.* 2001; Winocur *et al.* 2014). The area of the Frontal Cordillera to the east of the basement core is referred to here as the eastern Frontal Cordillera (Fig. 5). Finally, a NNE–SSW-trending magmatic belt of Eocene age intrudes the areas of the central and western Frontal Cordillera (Figs 2 & 5). South of 31.5°S, the area to the east of the main topographic front corresponds to the Principal Cordillera (Fig. 5), which is defined by a core of Oligocene–Miocene folded volcano-sedimentary rocks (Charrier *et al.* 2002; Mpodozis *et al.* 2009; Jara & Charrier 2014) flanked to the east by a fold-and-thrust belt of Mesozoic sedimentary and volcanic rocks (Fig. 5). These rocks are unconformably covered by Miocene subhorizontal volcanic rocks and intruded by a north–south-trending Miocene magmatic belt (Fig. 3; Mpodozis *et al.* 2009; Jara & Charrier 2014).

Crustal thickening processes in the study area began with the Late Cretaceous tectonic inversion of volcano-sedimentary extensional basins of a Lower Jurassic–Lower Cretaceous arc–back-arc system (Emparán & Pineda 2000; Arancibia 2004; Emparán & Pineda 2006; Charrier *et al.* 2007; Salazar 2012). Late Cretaceous inversion reactivated pre-existing normal faults along the Coastal and Frontal Cordilleras (Fig. 3; Emparán & Pineda 2000; Arancibia 2004; Emparán & Pineda 2006; Pineda & Emparán 2006; Arévalo *et al.* 2009). Eocene–Oligocene compression throughout the study area is associated with the Incaic Orogenic Phase (Steinmann 1929; Charrier & Vicente 1972; Cornejo *et al.* 2003). The Incaic Orogenic Phase corresponds to an important episode of shortening, uplift and exhumation widely recognized throughout the Domeyko Cordillera in northern Chile during the Eocene and Oligocene. Palaeomagnetic data indicate that Eocene–Oligocene clockwise palaeomagnetic rotations become mostly zero south of 31°S (Arriagada *et al.* 2009, 2013). Therefore, it has been interpreted that the study area includes the southern limit of Incaic deformation (Arriagada *et al.* 2009, 2013). According to structural and geochronological data, Eocene compression in the Huasco Valley was associated with inversion of previous Lower Cretaceous extensional basins by a series of low-angle faults located between the San Félix and La Totora Faults in the western and central Frontal Cordillera (Figs 3 & 5, Salazar 2012). At the latitude of the Elqui River

Fig. 2. (**a**) Shaded relief image map colour-coded for mean annual precipitation downloaded from http://climate.geog.udel.edu/~climate/html_pages/download.html. (**b**) Elevation map throughout study area based in the SRTM DEM. Dashed red lines mark the position of topographic fronts. Dashed blue lines mark the main rivers and tributaries. Dashed black line marks the international border. (**c**) Slope map throughout study area derived from the SRTM DEM. Thick dashed black line marks the position of the main topographic front. Thin dashed line marks the position of the international border. Arrows mark depressed areas within the Algarrobillo pediplain south of 30°S. (**d**) Maximum (red) and minimum (blue) elevation profiles in a 5 km diameter swath. Arrows mark the position of topographic fronts. Trace of profiles in Figure 2b.

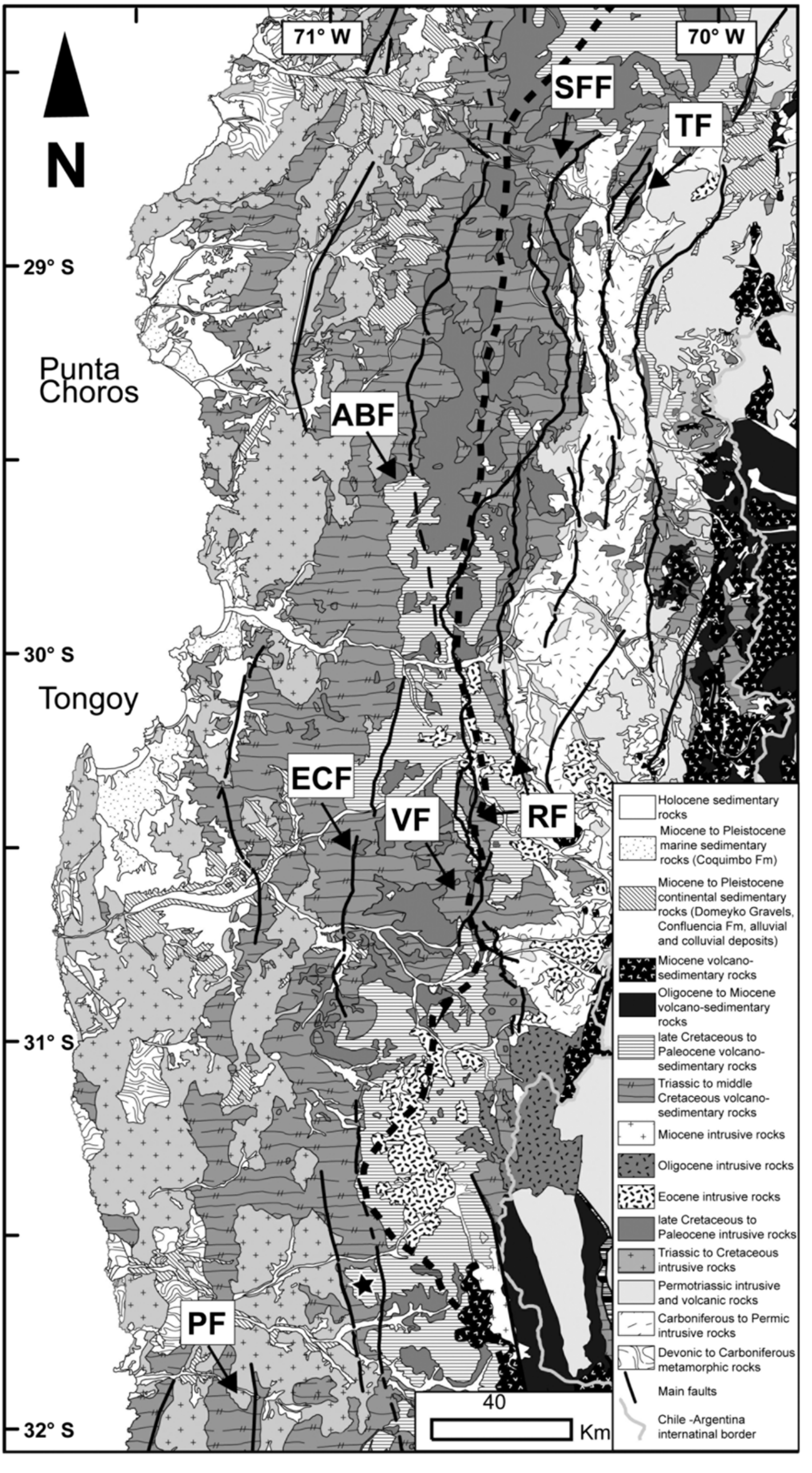
71° W
70° W
N
SFF
TF
29° S
Punta Choros
ABF
30° S
Tongoy
ECF
VF
RF
31° S
PF
32° S
40
Km
Holocene sedimentary rocks
Miocene to Pleistocene marine sedimentary rocks (Coquimbo Fm)
Miocene to Pleistocene continental sedimentary rocks (Domeyko Gravels, Confluencia Fm, alluvial and colluvial deposits)
Miocene volcano-sedimentary rocks
Oligocene to Miocene volcano-sedimentary rocks
late Cretaceous to Paleocene volcano-sedimentary rocks
Triassic to middle Cretaceous volcano-sedimentary rocks
Miocene intrusive rocks
Oligocene intrusive rocks
Eocene intrusive rocks
late Cretaceous to Paleocene intrusive rocks
Triassic to Cretaceous intrusive rocks
Permotriassic intrusive and volcanic rocks
Carboniferous to Permic intrusive rocks
Devonic to Carboniferous metamorphic rocks
Main faults
Chile -Argentina internatinal border

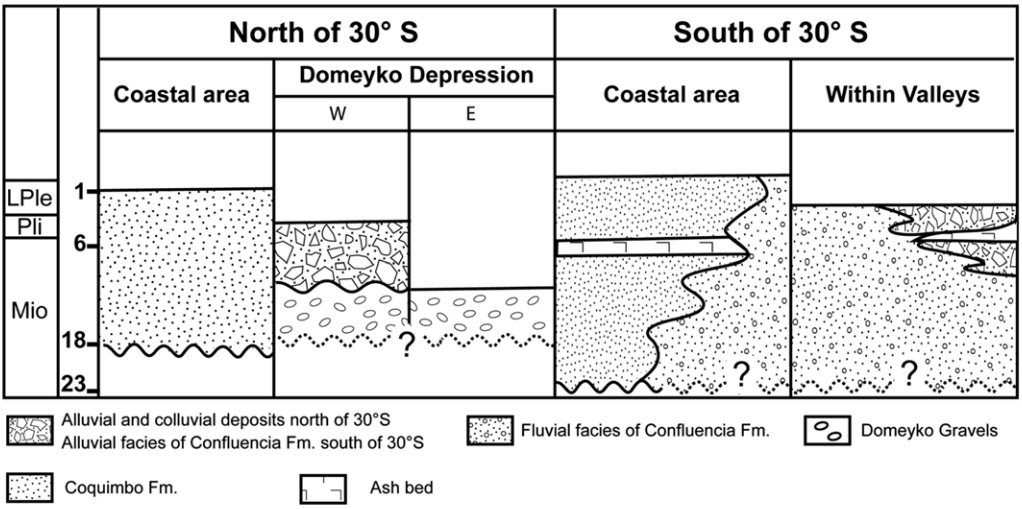

Fig. 4. Chronostratigraphic chart for Neogene and Quaternary sedimentary units exposed in the Coastal Cordillera north and south of 30°S. Mio, Miocene; Pli, Pliocene; LPle, Lower Pleistocene.

valley, the Eocene compression was related to a pop-up system formed by the closely spaced west-vergent Vicuña Reverse Fault and the east-vergent Rivadavia Reverse Fault in the western Frontal Cordillera (Figs 3 & 5). Finally, contractional tectonics affected the eastern Frontal Cordillera and the Principal Cordillera from the Early Miocene to at least the Late Miocene (Nasi *et al.* 1990; Rivano & Sepúlveda 1991; Bissig *et al.* 2001; Mpodozis *et al.* 2009; Winocur 2010; Jara & Charrier 2014; Winocur *et al.* 2014).

Large- to medium-scale geomorphological features

The topographic front that separates the Coastal Cordillera from the Frontal Cordillera defines two areas differing in their slope and hypsometry (Aguilar *et al.* 2013). The Frontal Cordillera presents contrasting slope values, with very high values (>45°) associated with canyons and low values (<20°) mostly observed at the high elevations of watersheds in the eastern Frontal Cordillera along the international border between Chile and Argentina (Fig. 2c). The Coastal Cordillera has homogeneous and lower slope values compared with the Frontal Cordillera, although high slope values are observed locally within river valleys and along the edges of low-slope areas (Fig. 2c). Another abrupt rise in the mean elevation present throughout west–east transects within the Coastal Cordillera defines a secondary topographic front (Fig. 2b). It is characterized by *c.* 600 to 1000 m of relief (difference in elevations) and separates the Coastal Cordillera into two areas referred to here as the western Coastal Cordillera and the eastern Coastal Cordillera (Fig. 5). Hypsometric integral values show a progressive increase from the Coastal Cordillera to the Frontal Cordillera, revealing that the zone between the secondary and main topographic fronts is an ancient mountain front, which probably evolved as a degradational feature carved during the Neogene (Aguilar *et al.* 2013). The low-slope areas throughout the Coastal and eastern Frontal Cordilleras are also generally characterized by low relief, forming sub-planar inter-river areas (i.e. the interfluves). These sub-planar surfaces resemble the morphology of palaeosurfaces widely described in the Central Andes forearc to the north and south of the study area (Mortimer 1973; Tosdal *et al.* 1984; Clark *et al.* 1990; Farías *et al.* 2005; García & Hérail 2005; Quang *et al.* 2005; Hoke *et al.* 2007; Riquelme *et al.*

Fig. 3. Geological map of the study area, based on Sernageomin (2003). The black dashed line marks the main topographic front line that separates the Coastal Cordillera to the west, from the Frontal Cordillera to the east. Black stars show location of tuffs dated by U–Pb zircon geochronology on top of the La Silla Pediplain and the Algarrobillo Pediplain in this study. VF, Vicuña Fault; RF, Rivadavia Fault; SFF, San Félix Fault; TF, La Totora Fault; ABF, Agua de los Burros Fault; ECF, El Chape Fault; PF, Pupio Fault.

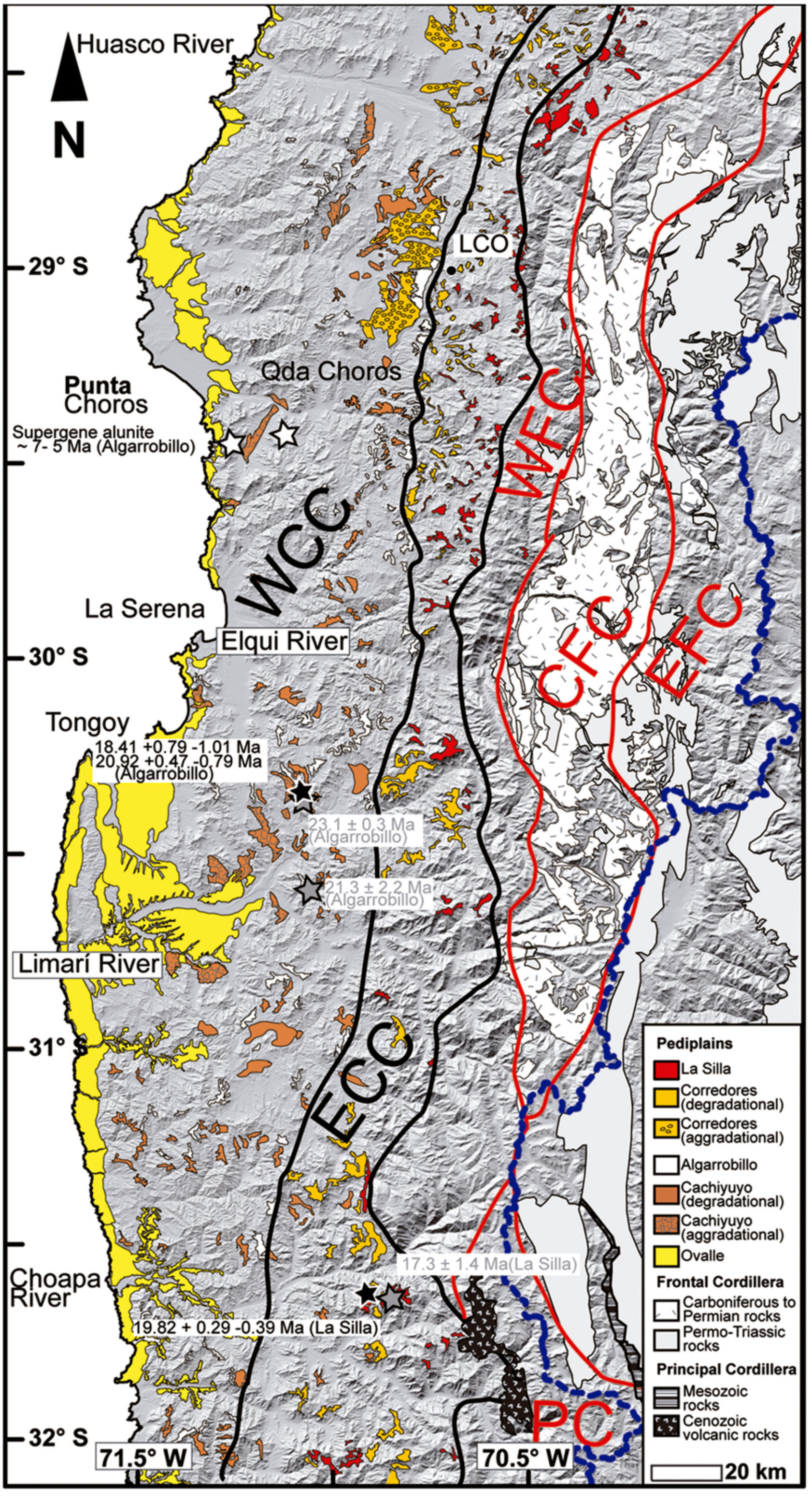
Huasco River
N
29° S
LCO
Qda Choros
Punta Choros
Supergene alunite
~ 7- 5 Ma (Algarrobillo)
WCC
WFC
CFC
EFC
La Serena
Elqui River
30° S
Tongoy
18.41 +0.79 -1.01 Ma
20.92 +0.47 -0.79 Ma
(Algarrobillo)
23.1 ± 0.3 Ma
(Algarrobillo)
21.3 ± 2.2 Ma
(Algarrobillo)
Limarí River
31° S
ECC
17.3 ± 1.4 Ma(La Silla)
Choapa River
19.82 + 0.29 -0.39 Ma (La Silla)
32° S
71.5° W
70.5° W
PC
Pediplains
La Silla
Corredores (degradational)
Corredores (aggradational)
Algarrobillo
Cachiyuyo (degradational)
Cachiyuyo (aggradational)
Ovalle
Frontal Cordillera
Carboniferous to Permian rocks
Permo-Triassic rocks
Principal Cordillera
Mesozoic rocks
Cenozoic volcanic rocks
20 km

2007; Farías *et al.* 2008*a*, *b*; Hall *et al.* 2008). Their low relief and slope indicate that incision was mostly inhibited during landform formation. However, their present-day location at hundreds of metres above the river thalwegs implies that they were initially graded to an ancient base level. Therefore, they are generally interpreted as palaeosurfaces displaced from their original location due to regional forearc uplift or tilting (Mortimer 1973; Tosdal *et al.* 1984; Farías *et al.* 2005; Hoke *et al.* 2007; Riquelme *et al.* 2007; Farías *et al.* 2008*a*, *b*). These types of sub-planar palaeosurfaces have been mostly classified as pediplains (Mortimer 1973; Tosdal *et al.* 1984), that is, extensive surfaces formed due to the coalescence of multiple pediments. Pediments correspond to abraded bedrock surfaces covered by a thin veneer of alluvial debris or weathered material (Cooke *et al.* 1993). It has been recognized that pediplains may contain degradational and aggradational counterparts, with degradational parts corresponding to bedrock surfaces and aggradational parts corresponding generally to the top surface of fluvial and/or alluvial deposits that represent the erosional material formed due to bedrock surface degradation (Mortimer 1973; Tosdal *et al.* 1984; Riquelme *et al.* 2003; Riquelme *et al.* 2007).

In the Coastal Cordillera of the study area, four to six pediplains have already been mapped in the area of the Domeyko Depression (Garrido 2009; Urresty 2009). South of 30°S, a geomorphological marker formed by marine and continental landforms that have been uplifted *c.* 150 m was dated using cosmogenic ^{10}Be (Rodríguez *et al.* 2013). The marine landforms correspond to shore platforms partly developed on top of the older Coquimbo Formation (Figs 3 & 4; Le Roux *et al.* 2006). The continental landforms correspond to a high strath terrace and a pediment that form a single continental planation surface mostly carved into older fluvial gravels from the Miocene to Pleistocene Confluencia Formation (Fig. 4; Emparán & Pineda 2006).

Pediplains have been identified throughout the western Frontal Cordillera (Aguilar *et al.* 2013) and were mapped and dated in the eastern Frontal Cordillera along the international border between Chile and Argentina (Bissig *et al.* 2002; Nalpas *et al.* 2009). No pediplains have been identified within the central Frontal Cordillera.

Here we have mapped pediplains mostly in the Coastal Cordillera (Figs 5 & 6a–c). Importantly, the present study is the first attempt to regionally map and correlate the pediplains of the Coastal and Frontal Cordilleras in north-central Chile in order to characterize the processes involved in their formation, uplift and incision.

Methods

Geomorphological mapping

Satellite images and elevation, slope and geological maps together with field observations were used to map pediplains. The satellite images used included the panchromatic band of the Landsat 7 ETM+ presenting a resolution of 15 m per pixel. Elevation and slope maps were extracted from the Shuttle Radar Topography Mission digital elevation model (SRTM DEM, 90 m resolution per pixel) using ArcGis 9.3 and Envi 4.2 software packages. The geological maps used range in scale between 1:250 000 and 1:100 000. Flow grids were extracted from the SRTM DEM using the software RiverTools to visualize the drainage network and the thalweg profiles of the main channels that incise the pediplains. In order to standardize the geomorphological mapping, criteria for surface recognition were defined, which are similar to a protocol used by Clark *et al.* (2006) to recognize remnant surfaces of an ancient landscape throughout the eastern Tibetan Plateau. As previously mentioned, the low relief and slope of the studied surfaces allow us to deduce that they formed graded to their respective original base-level surfaces. Therefore, in order to map these surfaces it was necessary to establish maximum values for relief and slope. The maximum relief for surface recognition was established as *c.* 600 m (Clark *et al.* 2006) whereas only surfaces presenting moderately low slopes (<20°) were mapped. It was also necessary to put some constraints on other geomorphological or sedimentological features of these surfaces that indicate they were actually displaced from their original base levels, as they lack significant active

Fig. 5. Remnants of pediplains throughout the study area in shaded relief image of the SRTM DEM. Black stars show location of tuffs dated by U–Pb zircon geochronology overlying the La Silla Pediplain in Cerro Carrizo and the Algarrobillo Pediplain in Quebrada Higuerillas. Grey stars show location of volcanic deposits overlying the La Silla and Algarrobillo Pediplains dated in previous studies (Rivano & Sepúlveda 1991; Bissig 2001; Emparán & Calderón 2008). White stars show location of supergene alunite samples dated by ^{40}Ar/^{39}Ar geochronology by Creixell *et al.* (2012). Black lines mark the position of topographic fronts. Red lines mark the boundaries between the different blocks composing the Frontal Cordillera. The blue dashed line marks the international border between Chile and Argentina. WCC, western Coastal Cordillera; ECC, eastern Coastal Cordillera; WFC, western Frontal Cordillera; CFC, central Frontal Cordillera; EFC, eastern Frontal Cordillera; PC, Principal Cordillera; LCO, Las Campanas Astronomical Observatory.

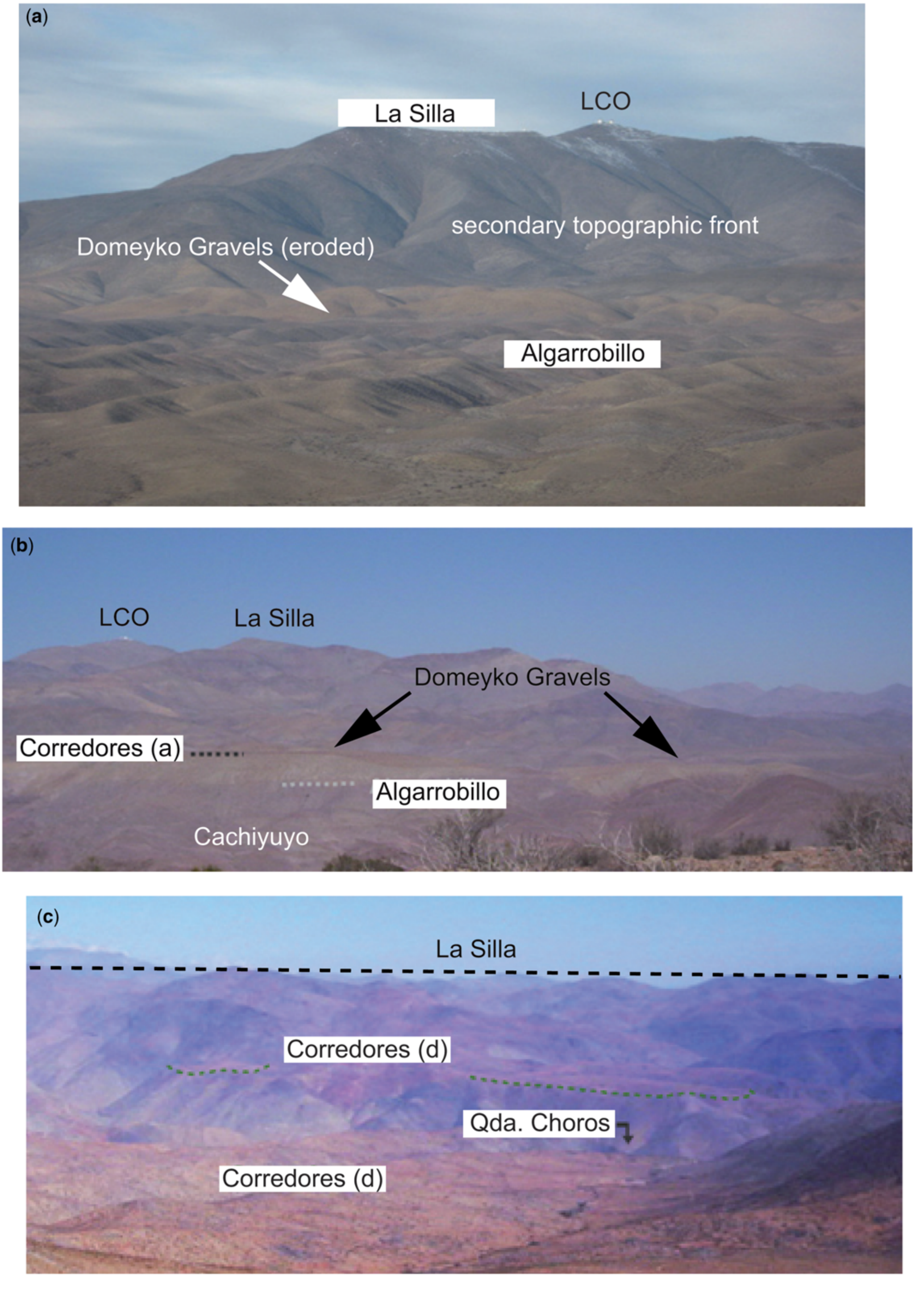

Fig. 6. (**a**) View to the NE of the secondary topographic front in the area of the Domeyko Depression. The Las Campanas Astronomical Observatory (LCO) (*c.* 2300 m a.s.l.) is observed on top of remnants of the La Silla Pediplain. LCO location in Figure 5. Remnants of the Algarrobillo Pediplain are exposed at the foot of the secondary topographic front underlying eroded exposures of the Domeyko Gravels. (**b**) View to the east of the secondary topographic front in

sedimentation, and that they are related to knick points downstream (Clark *et al.* 2006).

Geochronology

Three samples from tuff layers covering two different bedrock pediplains presented in the following section, the La Silla and the Algarobillo Pediplains, were collected from the localities of Cerro Carrizo and Quebrada Higuerillas (Fig. 7). The samples were crushed and sieved to obtain the 250–1000 μm fraction. Mineral separation was obtained according to standard laboratory techniques in the Mineral Separation Laboratory of the Geology Department of the University of Chile. At least 50 zircons from each sample were mounted in epoxy and polished for laser ablation analyses at the University of Arizona. The U–Pb geochronology of zircons was carried out using laser ablation-multicollector-inductively coupled plasma-mass spectrometry (LA-MC-ICP-MS) at the Arizona LaserChron Center (University of Arizona). Ages were calculated using the subroutine 'Zircon Age extractor' of Isoplot (Ludwig 2009), which implements an algorithm ('TuffZirc') for extracting reliable ages and age errors from suites of $^{238}U-^{206}Pb$ dates on complex single-zircon populations to finally provide a best estimate for the magmatic age of the tuff (Fig. 7).

Results

The pediplains studied here correspond to gently undulating bedrock and aggradational surfaces, which are exposed as patches that can be correlated based on their elevation and lateral connection. Furthermore, the pediplains had to meet the criteria defined in the previous section. A total of five levels of pediplains are recognized within the study area (Figs 5 & 8a, b). These five levels are systematically observed throughout the entire study area, but they display some differences between the regions located to the north and to the south of 30°S (Fig. 5). The two highest degradational pediplains, here named as La Silla and Corredores Pediplains, are located in the eastern Coastal Cordillera just to the east of the secondary topographic front (Figs 5 & 8a, b). The Corredores Pediplain is also composed of an aggradational part exposed within the western Coastal Cordillera just to the west of the secondary topographic front north of 30°S (Figs 5 & 8a). The Algarrobillo Pediplain is exposed within the western Coastal Cordillera just to the west of the secondary topographic front

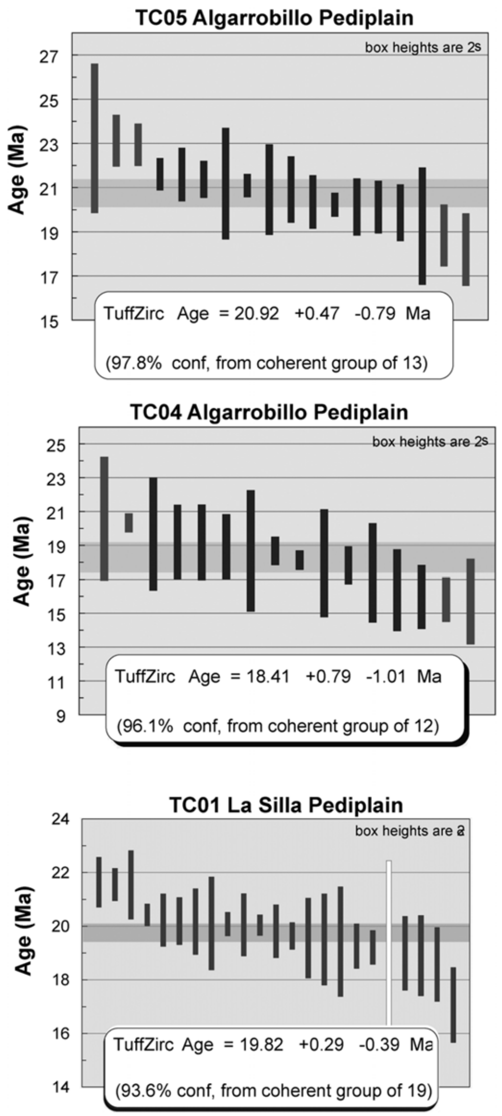

Fig. 7. LA-ICPMS U–Pb zircon ages obtained for tuffs covering the Algarrobillo and La Silla Pediplains. Errors are $\pm 2\sigma$.

Fig. 6. (*Continued*) the area of the Domeyko Depression. The LCO (*c.* 2300 m a.s.l.) is observed on top of remnants of the La Silla Pediplain. Remnants of the aggradational part of the Corredores Pediplain (Corredores (a) on top of the Domeyko Gravels) are exposed at the foot of the secondary topographic front. Remnants of the Algarrobillo Pediplain underlying the Domeyko Gravels are also observed. (**c**) View to the SE of remnants of the degradational part of the Corredores (Corredores (d)) Pediplain at both flanks Quebrada Choros.

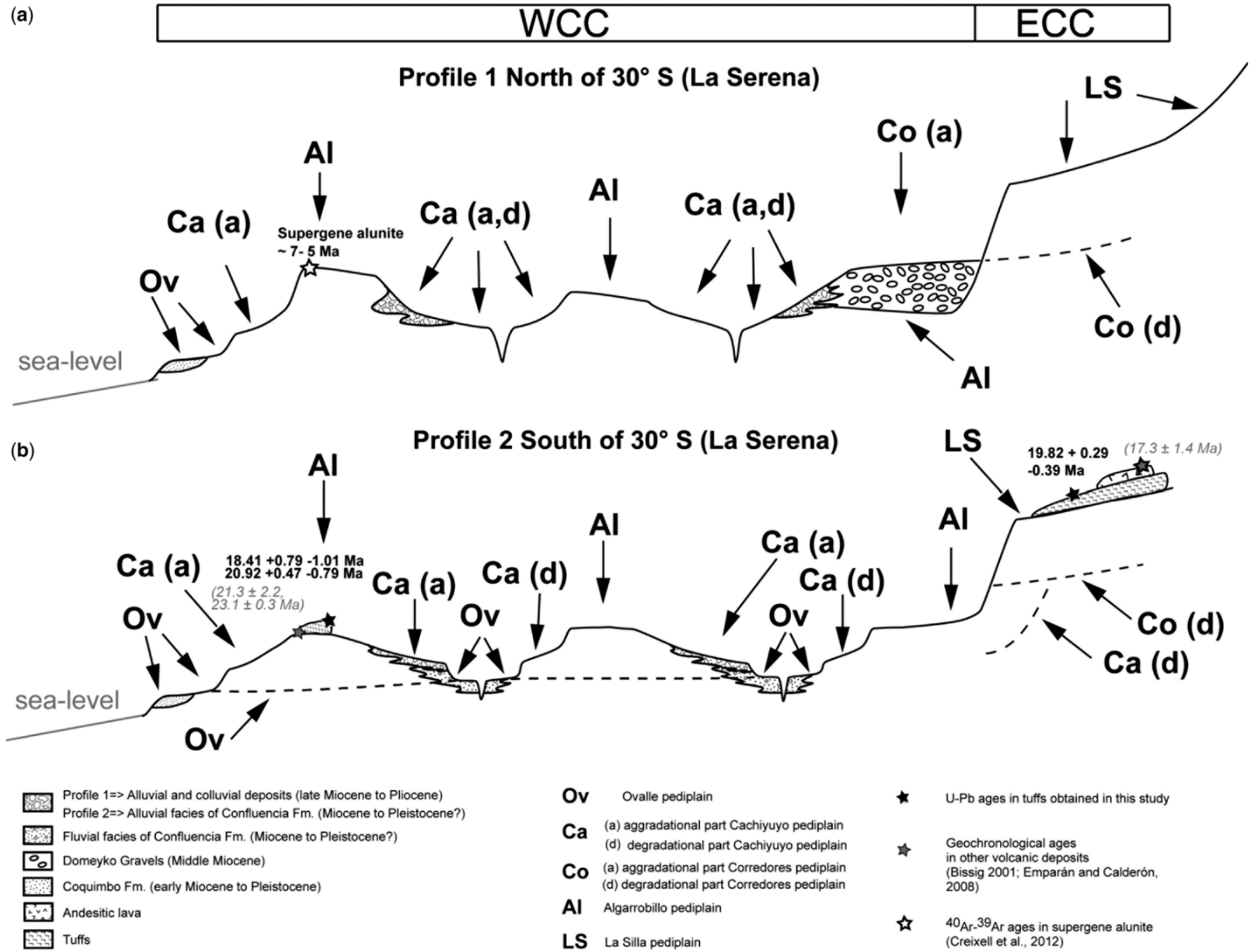

Fig. 8. (**a**) Schematic profiles of pediplains from the Coastal Cordillera north of 30°S. (**b**) Schematic profiles of pediplains from the Coastal Cordillera south of 30°S.

(Figs 5 & 8a, b). The Algarrobillo Pediplain underlies the aggradational deposits related to the development of the Corredores Pediplain north of 30°S (Figs 5, 6a, b & 8a). The Cachiyuyo Pediplain, which has a lower elevation in relation to the Algarrobillo Pediplain, is exposed in both the western and eastern Coastal Cordillera (Figs 5 & 8a, b). It presents both degradational and aggradational counterparts (Figs 5 & 8a, b). Finally, the lowest pediplain observed within the study area, the Ovalle Pediplain, occurs within the western Coastal Cordillera (Figs 5 & 8a, b).

La Silla Pediplain

The La Silla Pediplain corresponds to a degradational bedrock surface always exposed just to the east of the secondary topographic front (Figs 5, 6a–c & 8a, b). North of 30°S the pediplain is present in the eastern Coastal Cordillera and in some areas of the western Frontal Cordillera (Fig. 5). South of 30°S the pediplain forms the highest summits of the eastern Coastal Cordillera (Figs 5 & 8b). The range of elevations of the La Silla Pediplain is constant throughout the study area, lying between 3200 and 1800 m a.s.l. It is carved independent of the lithology into Upper Cretaceous and Paleocene volcano-sedimentary rocks and Paleocene–Eocene granitoids. Importantly, remnants of the La Silla Pediplain are exposed both west and east of the Vicuña Fault near the town of Hurtado (Fig. 9). The youngest rocks cross-cut by the La Silla Pediplain correspond to a granitoid with a U–Pb zircon age of 48.1 $\pm$ 0.4 Ma (Table 1; Emparán & Pineda 2006). One tuff sample interpreted as an ash fall overlying the La Silla Pediplain within the Choapa Valley was collected (Figs 5, 7 & 8b). The U–Pb zircon age obtained for this tuff sample is 19.82 + 0.29–0.39 Ma (Table 1; Figs 5, 7 & 8b). Additionally, an andesitic lava with a K–Ar age of 17.3 $\pm$ 1.4 Ma covers the dated tuff *c.* 2 km south of the sampled site and within the same surface remnant (Table 1; Figs 5 & 8b; Rivano & Sepúlveda 1991).

Corredores Pediplain

The Corredores Pediplain is composed of both degradational and aggradational counterparts (Figs 5, 6b, c & 8a, b). Its degradational part is a bedrock surface only exposed in the eastern Coastal Cordillera and always incised into the La Silla Pediplain (Figs 5 & 6c). The elevation of this bedrock surface ranges between 2000 and 1200 m a.s.l. throughout the entire study area. Similar to the La Silla Pediplain, it is mainly carved into the Upper Cretaceous and Paleocene volcano-sedimentary rocks, but it is also well developed on top of Paleocene granitoids. The aggradational part of the Corredores Pediplain is exposed to the west of the secondary topographic front and only in the area located to the north of 30°S, within the Domeyko Depression (Figs 5, 6b & 8a). It has an elevation range between 1400 and 800 m a.s.l., corresponding to the surface on top of the alluvial deposits of the Domeyko Gravels of probable Middle Miocene age (Table 1; Figs 5, 6b & 8a). Importantly, the aggradational part of the Corredores Pediplain is not observed south of 30°S (Figs 5 & 8b).

Algarrobillo Pediplain

The Algarrobillo Pediplain is a degradational bedrock surface that is separated by the secondary topographic front from the La Silla Pediplain and the degradational part of the Corredores Pediplain throughout the entire study area (Figs 5, 6a & 8a, b). North of 30°S, remnants of the Algarrobillo Pediplain are exposed on top of the NNE–NNW-trending ranges of the Coastal Cordillera and within the Domeyko Depression (Fig. 5). Remnants exposed at the summits of the NNE–NNW-trending ranges have elevations as high as 1800 m a.s.l. that diminish seawards to 1200 m a.s.l. Within the Domeyko Depression the elevation of the Algarrobillo Pediplain is *c.* 1700 m a.s.l. at the foothills of the secondary topographic front just north of 30°S. Further north it diminishes to 1200 m a.s.l. and plunges underneath the Domeyko Gravels of probable Middle Miocene age (Figs 5, 6a, b & 8a). Remnants of the Algarrobillo Pediplain at the western border of the Domeyko Depression are at elevations that are slightly lower (*c.* 1500–1200 m a.s.l.), but within the same elevation range as those on top of the NNE–NNW-trending ranges (*c.* 1800–1200 m a.s.l.). As no dislocation or encasement is observed between low relief/slope remnant surfaces of both areas, they are correlated here as part of the same original pediplain. South of 30°S, the Algarrobillo Pediplain's remnants form the summits of the western Coastal Cordillera in a range of elevations between 1600 and 1100 m a.s.l. that diminish progressively seawards. Here, exposures of the Algarrobillo Pediplain are present as close as *c.* 3 km to the present-day coastline (Fig. 5). The Algarrobillo Pediplain is carved mainly into Jurassic and Lower Cretaceous volcano-sedimentary and intrusive rocks. Two samples were collected from an ignimbritic deposit at the top of the Algarrobillo Pediplain (Figs 5, 7 & 8b). The U–Pb zircon geochronological determinations for these samples give two similar ages of 20.92 + 0.47–0.79 Ma and 18.41 + 0.79–1.01 Ma (Figs 5, 7 & 8b). In other studies two ages of 23.07 $\pm$ 0.33 ($^{40}Ar/^{39}Ar$ biotite) and 21.3 $\pm$ 2.2 (K–Ar biotite) were obtained for tuffs overlying

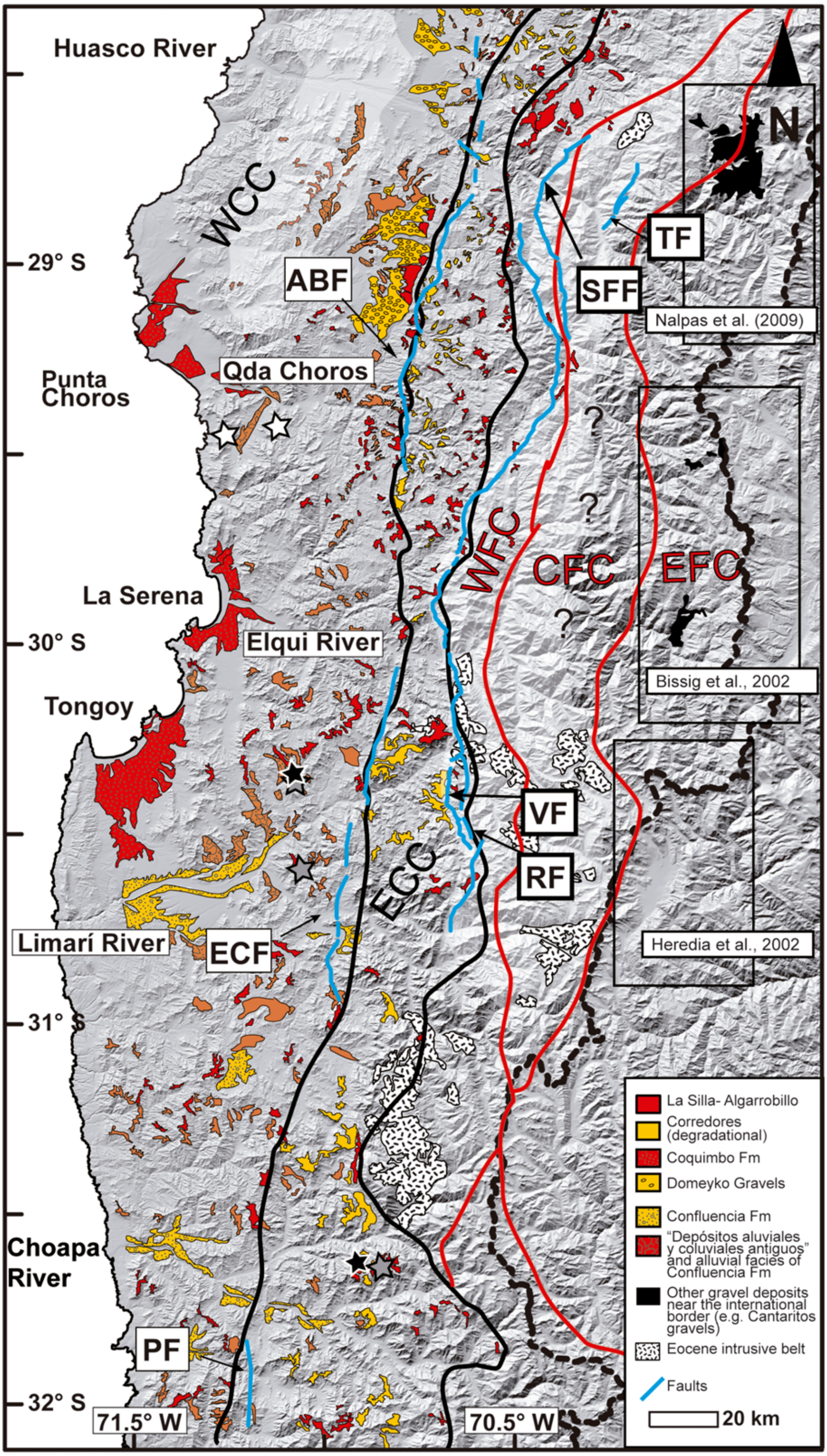

Huasco River
WCC
29° S
ABF
Punta Choros
Qda Choros
La Serena
30° S
Elqui River
Tongoy
Limarí River
ECF
ECC
31° S
Choapa River
PF
32° S
71.5° W
70.5° W
WFC
CFC
EFC
SFF
TF
VF
RF
N
Nalpas et al. (2009)
Bissig et al., 2002
Heredia et al., 2002
La Silla- Algarrobillo
Corredores (degradational)
Coquimbo Fm
Domeyko Gravels
Confluencia Fm
"Depósitos aluviales y coluviales antiguos" and alluvial facies of Confluencia Fm
Other gravel deposits near the international border (e.g. Cantaritos gravels)
Eocene intrusive belt
Faults
20 km

the Algarrobillo Pediplain just to the south of La Serena (Table 1; Figs 5 & 8b; Bissig 2001; Emparán & Calderón 2008).

Cachiyuyo Pediplain

The Cachiyuyo Pediplain is composed of both aggradational and degradational bedrock counterparts (Figs 5 & 8a, b). They are incised within north–south-trending tributaries draining the Algarrobillo and Corredores Pediplains (Figs 5 & 8a, b). The elevation of the Cachiyuyo Pediplain mostly ranges between 1000 and 700 m a.s.l. north of 30°S and between 1100 and 500 a.s.l. south of 30°S. The degradational part of the Cachiyuyo Pediplain is carved mainly into Jurassic– Lower Cretaceous volcano-sedimentary and intrusive rocks and to a lesser degree into the Triassic succession of volcanic rocks and the Palaeozoic metamorphic basement. Within the Domeyko Depression the aggradational part of the Cachiyuyo Pediplain corresponds to the surface on top of alluvial and colluvial sediments of probable Late Miocene–Pliocene age (Table 1; Figs 8a & 9; Arévalo *et al.* 2009). South of 30°S, the aggradational part of the Cachiyuyo Pediplain corresponds to the surface on top of the alluvial facies within the Confluencia Formation (Table 1; Figs 8b & 9; Emparán & Pineda 2006), correlated with the alluvial and colluvial deposits exposed to the north of 30°S. In both areas the alluvial and colluvial deposits are adjacent to topographically higher areas corresponding mostly to remnants of the Algarrobillo and the aggradational part of the Corredores Pediplains (Fig. 8a, b).

Ovalle Pediplain

The Ovalle Pediplain is exposed south of 30°S as a single planation surface formed by morphologically continuous marine and continental landforms already described and dated using cosmogenic ^{10}Be (Rodríguez *et al.* 2013). These ^{10}Be cosmogenic age determinations indicate that the Ovalle Pediplain formed between *c.* (1200?) 800 and 500 ka (Early–Middle Pleistocene, Table 1). Its elevation varies from *c.* 100 m a.s.l. near the coast to *c.* 400 m a.s.l. near the secondary topographic front. The Ovalle Pediplain is incised into the Algarrobillo and Cachiyuyo Pediplains (Figs 5 & 8a, b) and has been uplifted *c.* 150 m above the present-day thalwegs (Rodríguez *et al.* 2013). Whereas the marine landforms mainly correspond to a wide shore platform, the continental landforms correspond to a high fluvial terrace and a pediment morphologically connected and systematically exposed throughout the lower and middle courses of present-day river valleys in the area south of 30°S (Figs 5 & 8b, Rodríguez *et al.* 2013). In this area, the Ovalle Pediplain cross-cuts Jurassic granitoids and the Palaeozoic metamorphic basement, and the older alluvial and fluvial facies of the Confluencia Formation within the valleys. According to the interpretation of the concentration of cosmogenic ^{10}Be in samples from the high fluvial terrace, this landform corresponds to an older aggradational terrace related to fluvial deposition of the Confluencia Formation later modified during the pedimentation event leading to the development of the Ovalle Pediplain (Rodríguez *et al.* 2013). North of 30°S the Ovalle Pediplain is restricted to the coastal region (Figs 5& 8a) where it is exposed as a wide shore platform or *rasa* (Regard *et al.* 2010). Near the coast in both areas, the shore platform is carved into Jurassic and Triassic granitoids, the Miocene–Pleistocene marine deposits of the Coquimbo Formation (Fig. 8a, b) and the Palaeozoic metamorphic basement.

Discussion

Age of formation and incision of pediplains

The age of pediplains is generally constrained by the youngest geological unit overlain by the pediment and the geological units covering the surface

Fig. 9. Shaded relief image of the study area showing the trace of main faults and showing remnants of the Corredores and Algarrobillo Pediplains, as well as outcrops of Lower Miocene–Pleistocene continental and marine deposits. Black stars show location of tuffs dated by U–Pb zircon geochronology overlying the La Silla Pediplain in Cerro Carrizo and the Algarrobillo Pediplain in Quebrada Higuerillas. Grey stars show location of volcanic deposits overlying the La Silla and Algarrobillo Pediplains dated in previous studies (Rivano & Sepúlveda 1991; Bissig 2001; Emparán & Calderón 2008). White stars show location of supergene alunite samples dated by ^{40}Ar/^{39}Ar geochronology by Creixell *et al.* (2012). Black lines mark the position of topographic fronts. Red lines mark the boundaries between the different blocks composing the Frontal Cordillera. Blue lines mark the trace of main faults. The areas in transparent white indicate the probable extension of an Eocene positive relief in the western Coastal Cordillera and of the Main Incaic Range along the western and central Frontal Cordillera. WCC, western Coastal Cordillera; ECC, eastern Coastal Cordillera; WFC, western Frontal Cordillera; CFC, central Frontal Cordillera; EFC, eastern Frontal Cordillera; ABF, Agua de los Burros Fault; ECF, El Chape Fault; PF, Pupio Fault; VF, Vicuña Fault; RF, Rivadavia Fault; SFF, San Félix Fault; TF, La Totora Fault.

Table 1. *Geochronological and relative ages used to constrain the development of pediplains from the Coastal Cordillera in north-central Chile (28–32°S)*

	Name	Location*	Description	Geochronological constraints
+	La Silla	ECC (some areas of WFC)	Degradational	Andesitic lava (other studies) =>17.3 ± 1.4 Ma (K–Ar whole rock) overlying tuffs (this study) =>19.82 +0.29 −0.39 Ma (U–Pb zircon) youngest rocks cross-cut (other studies) => 48.1 ± 0.4 Ma U–Pb zircon
	Corredores	ECC	Degradational and aggradational (Domeyko Gravels)	Probable Middle Miocene age for Domeyko Gravels => probable Late Miocene age for Corredores Pediplain
Elevation	Algarrobillo	WCC	Degradational	Supergene alunite (incision timing) =>*c.* 7–5 Ma ^{40}Ar/^{39}Ar overlain by Domeyko Gravels overlying tuffs (this study) =>20.92 + 0.47 −0.79 Ma and 18.41 + 0.79 − 1.01 Ma (U–Pb zircon) overlying tuffs (other studies) => 23.07 ± 0.33 (^{40}Ar /^{39}Ar biotite) and 21.3 ± 2.2 Ma (K–Ar biotite)
	Cachiyuyo	WCC (some areas of the WFC)	Degradational and aggradational (alluvial facies of Confluencia Fm and Depósitos aluviales and coluviales antiguos)	Probable Late Miocene–Early Pliocene age for 'Depósitos aluviales and coluviales antiguos' => probable Late Pliocene age for Cachiyuyo Pediplain
−	Ovalle	WCC	Degradational	^{10}Be cosmogenic ages point to a formation period between *c.* (1200?) 800 and 500 ka (Rodríguez *et al.* 2013)

*ECC, eastern Coastal Cordillera; WCC, western Coastal Cordillera; WFC, western Frontal Cordillera.

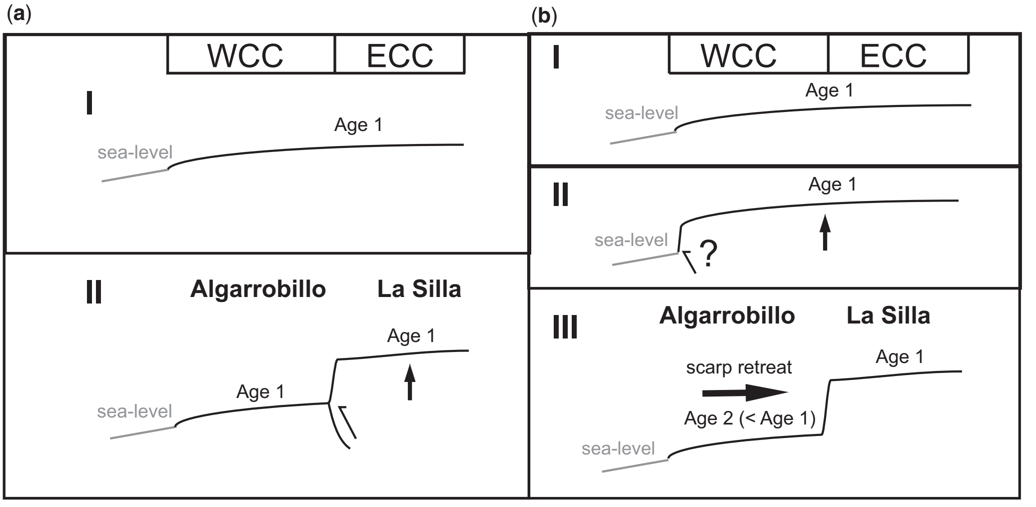

Fig. 10. Schematic profiles showing possible origins for the original La Silla–Algarrobillo pediplain. (**a**) Original La Silla–Algarrobillo pediplain forming near sea-level and offset by north–south-trending faults aligned with the secondary topographic front. (**b**) Original La Silla–Algarrobillo pediplain forming near sea-level with the secondary topographic front forming due to scarp retreat.

(e.g. Bissig *et al.* 2001). Whereas the age of the youngest geological unit eroded by the pediment constrains the maximum age of initiation of pediplain development, the ages of the oldest units covering this surface are used to constrain the minimum age of development of the pediplain. Finally, it is also important to consider the relative ages given by the relationship of incision between two pediplains (Table 1).

Regardless of the mechanism by which the tuffs were deposited on top of the Algarobillo and La Silla Pediplains, the ages obtained (Table 1) indicate that both surfaces were sub-planar components of the landscape by the Early Miocene. However, it is known that ignimbritic flows or ash falls are able to surge up valley flanks. This could imply that the Algarobillo and La Silla Pediplains were not necessarily graded to base level when the tuffs were deposited on top. The La Silla Pediplain is also covered by an andesitic lava of *c.* 17 Ma (Table 1; Figs 5 & 8b; Rivano & Sepúlveda 1991). As lava is not able to surge up valley flanks, the La Silla Pediplain was graded to its base level when both deposits covered this surface. The Early Miocene ages of several tuffs (Table 1; Figs 5 & 8b) covering the Algarrobillo Pediplain are in good agreement with the underlying position of this surface with respect to the Domeyko Gravels of probable Middle Miocene age within the Domeyko Depression (Fig. 8a). The fact that the Algarrobillo Pediplain served as a depocentre for the Domeyko Gravels also suggests that it was graded to its base level by the Early Miocene, just before deposition of this unit. Importantly, exposures of the La Silla Pediplain are systematically separated from the Algarrobillo Pediplain remnants by a secondary topographic front (Fig. 8a, b). This scarp could present two different origins. One implies that both pediplains formed a once-continuous surface that was displaced after *c.* 17 Ma by a series of north–south faults, namely, the Agua de los Burros, El Chape and Pupio Faults (Fig. 10a; Moscoso *et al.* 1982; Rivano & Sepúlveda 1991; Pineda & Emparán 2006; Arévalo *et al.* 2009), which are spatially correlated with the secondary topographic front (Fig. 9). The other possibility is that this feature results from scarp retreat after regional uplift of a single surface (Fig. 10b). In such a case, the La Silla Pediplain would be older than the Algarrobillo Pediplain (Fig. 10b). However, the ages between *c.* 23 and 18 Ma of tuffs overlying the Algarrobillo Pediplain are slightly older than the age of *c.* 19 to 17 Ma of volcanic deposits overlying the La Silla Pediplain. Therefore, the geomorphological and geochronological data described here strongly suggest that the La Silla and Algarrobillo Pediplains once formed a single low-relief/slope surface that was later offset by north–south faults that displaced the La Silla Pediplain to higher elevations (Fig. 10a). According to the estimated age of the Domeyko Gravels, offset from the original La Silla–Algarrobillo single surface would have occurred after *c.* 17 Ma and prior to the Middle Miocene. After the offset of this original surface, the degradational and aggradational parts of the Corredores Pediplain developed on top of the

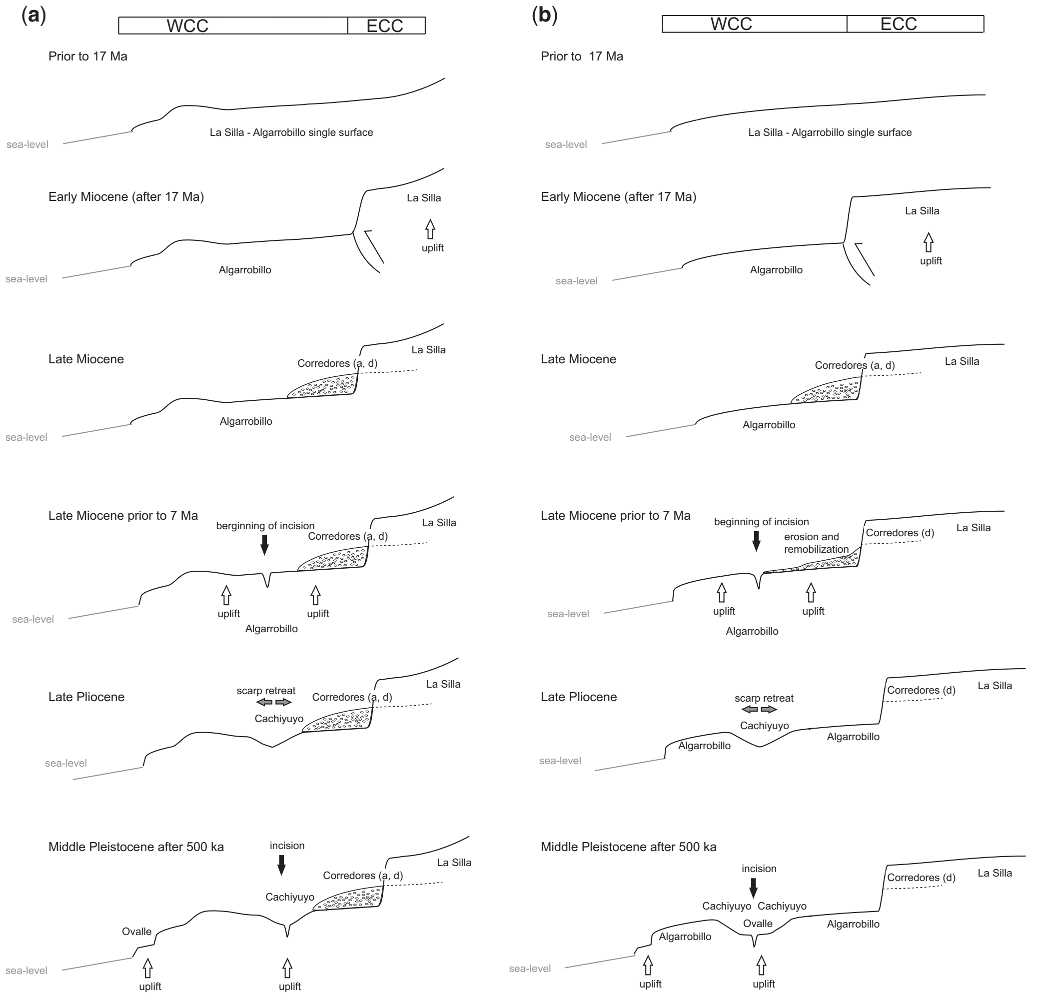

Fig. 11. Landscape evolution model for the Coastal Cordillera from the Early Miocene to the Middle Pleistocene: (**a**) north of 30°S; and (**b**) south of 30°S. WCC, western Coastal Cordillera: ECC, eastern Coastal Cordillera.

La Silla and Algarrobillo Pediplains, respectively (Fig. 11a, b). According to the probable Middle Miocene age of the Domeyko Gravels, the Corredores Pediplain was already formed by the Late Miocene (Table 1; Fig. 11a, b). Presently the Corredores Pediplain's remnants are located several hundreds of metres above the river thalwegs (Fig. 8a, b). Similarly, the Algarrobillo Pediplain's remnants, which underlie the aggradational part of the Corredores Pediplain (Fig. 8a, b), are also located several hundreds of metres above the present-day river's thalwegs (Fig. 8a, b). Thus, both surfaces were incised after the Late Miocene (Fig. 11a, b). A maximum age for incision of the Algarrobillo and Corredores Pediplains is given by the age of the Cachiyuyo Pediplain. The estimated age for the alluvial to colluvial deposits related to the aggradational part of the Cachiyuyo Pediplain is Late Miocene–Early Pliocene (Table 1). Thus, the age of the Cachiyuyo Pediplain is younger than Early Pliocene, probably Late Pliocene (Table 1). Supergene alunite $^{40}Ar/^{39}Ar$ ages in the range *c.* 7 to 5 Ma were obtained from samples collected from the Algarrobillo Pediplain and valleys incising this surface near Quebrada Choros (Table 1; Figs 5 & 8a; Creixell *et al.* 2012). Episodes of supergene copper enrichment are thought to occur under semi-arid conditions beneath pediplains due to abrupt descents in the water table and concomitant pediment incision (Sillitoe *et al.* 1968; Mortimer 1973; Tosdal *et al.* 1984; Quang *et al.* 2005). It is not clear if such abrupt descents are related to tectonic uplift (Mortimer 1973) or to changing climatic conditions (Arancibia *et al.* 2006). Regardless of the cause of water table descents, the ages of supergene alunite are consistent with incision of the Algarrobillo Pediplain taking place between *c.* 7 and 5 Ma (Late Miocene–Early Pliocene, Table 1), shortly before the development of the Late Pliocene Cachiyuyo Pediplain (Table 1). Finally, the ^{10}Be cosmogenic age determinations made by Rodríguez *et al.* (2013) indicate the Ovalle Pediplain formed between *c.* (1200?) 800 and 500 ka (Early–Middle Pleistocene, Table 1).

In the eastern Frontal Cordillera near the international border between 29 and 30°S at the head of the Huasco River, three once-continuous levels of pediplains are well preserved (Bissig *et al.* 2002). The higher pediplain, the Frontera–Deidad surface (4600–5300 m a.s.l.), intersects intrusive bodies with an ^{40}Ar/^{39}Ar age of *c.* 18 Ma (Bissig *et al.* 2002), which constrains its maximum age. The minimum age of this surface is inferred to be 15 Ma (Bissig *et al.* 2002). Farther north within the Huasco River's headwaters a smooth surface (4350–4500 m a.s.l.) is defined by the top of a package of gravels, informally named the Cantarito gravels, previously correlated with the Atacama Gravels (Fig. 9; Cancino 2007) exposed within the Central Depression at 27°S (Mortimer 1973). This surface probably corresponds to the aggradational part of the Frontera–Deidad surface as an ignimbrite at the base of the gravels was dated at 22 ± 0.6 Ma (K–Ar, Cancino 2007). Entrenched into the Frontera–Deidad surface, that of the Azufrera–Torta is observed (4300–4600 m a.s.l.). The minimum age of the Azufrera–Torta surface is constrained by an overlying dacitic tuff with an ^{40}Ar/^{39}Ar age *c.* 12.7 Ma (Bissig *et al.* 2002). Finally, the pedimentation process finished with the incision of the palaeovalley formed by the Los Rios surface, whose minimum age is defined by an ignimbrite on top presenting an ^{40}Ar/^{39}Ar age of *c.* 6 Ma (Bissig *et al.* 2002). The few peaks that arise on top of the Frontera–Deidad surface would correspond to vestiges of an older uplifted surface, the Cumbre surface, which represents a local back-scarp of the Frontera–Deidad surface (Bissig *et al.* 2002). According to the rocks that cross-cut this surface and its relationship with the Frontera–Deidad surface (Bissig *et al.* 2002), the probable age of the Cumbre surface is Late Oligocene–Early Miocene. Between 30 and 31°S, Heredia *et al.* (2002) recognized an extensive planation surface on top of rocks of the Permo-Triassic basement and covered by Early Miocene lavas (*c.* 18 Ma), which may also be correlated with the Cumbre surface surface (Fig. 9).

Independently of the mechanisms involved in pediplain development at both locations, the similarity between the ages presented here and the ages obtained by Bissig *et al.* (2002) indicates that tectonic and climatic conditions were favourable for pediplain formation in the Coastal and in the eastern Frontal Cordillera since the Early Miocene. A priori, some chronological correlations among the pediplains from both areas can be suggested based on the age information and regional correlations given here. The Early Miocene minimum age of the original La Silla–Algarrobillo pediplain indicates that this surface formed coevally with the Late Oligocene–Early Miocene Cumbre surface. Deposition of the Domeyko Gravels and the development of the probable Late Miocene Corredores Pediplain would have outlasted the formation of both, the Frontera-Deidad and the Azufrera-Torta Pediplains, which formed after the Early Miocene (*c.* 22–18 Ma) and during the Late Miocene (*c.* 12 Ma), respectively. Importantly, the timing of incision of the Algarrobillo Pediplain (*c.* 7–5 Ma) coincides with the incision of the palleovalley of the Los Rios surface (*c.* 6 Ma). Finally, the age correlations between pediplains from the western Coastal Cordillera and the eastern Frontal Cordillera made here are only preliminary as further geomorphological and geochronological data are needed to support these correlations.

Location of pediplains with respect to the Incaic Range

Taking the constraints on Eocene–Oligocene upper plate deformation as indicators of the Incaic Range (see Regional Framework), we suggest that within the Huasco Valley the Incaic Range formed a NNE–NNW-trending belt between the San Félix and La Totora Faults in the western and central Frontal Cordillera (Salazar 2012) (Fig. 9). Within the Elqui and the northern Limarí Valleys, constraints on Eocene deformation and exhumation (Cembrano *et al.* 2003) indicate that the Incaic Range was shifted to the west with respect to further north. Here, mountain building during the Eocene would have been mostly focused in the area between the Vicuña and Rivadavia Faults (Fig. 9; Cembrano *et al.* 2003; Emparán & Pineda 2006; Pineda & Calderón 2008). However, exposures of Late Eocene–Early Oligocene arc-like stocks (Bocatoma unit, Mpodozis & Cornejo 1988) are observed further to the east (Fig. 9). The geochemical signature of these rocks indicates that they developed in a compressional-arc tectonic regime (Bissig *et al.* 2003). Thus, the Incaic Range probably extended further to the east in this area (Fig. 9), occupying the present-day western and central Frontal Cordilleras. To the south of 31°S, no evidence of Eocene–Oligocene contractional deformation is reported along Frontal/Principal Cordilleras of the Choapa Valley (Fig. 9). Importantly, apatite fission-track and U–Th/He thermochronology indicate that rocks from the Coastal Cordillera to the west of the Domeyko Depression to the north of 30°S were exhumed in response to uplift by the Middle to Late Eocene (Maksaev *et al.* 2009). In contrast, to the south of 30°S, apatite fission-track ages between *c.* 120 and 80 Ma in the western Coastal Cordillera (Cembrano *et al.* 2003) indicate that this area was exhumed in response to uplift by the Early to Late Cretaceous, prior to the Incaic Orogenic Phase. Thus, the Eocene–Oligocene palaeotopography along the study region was characterized by the presence of a Main Incaic Range along the western and central Frontal Cordilleras to the north of 31°S, but also by the presence of a positive relief in the western Coastal Cordillera to the west of the Domeyko Depression to the north of 30°S (Fig. 9). No evidence exists of the presence of an Eocene–Oligocene mountainous range along the Frontal/Principal Cordilleras south of 31°S nor the western Coastal Cordillera to the south of 30°S (Fig. 9).

The mentioned constraints on Eocene to Oligocene contractional deformation and exhumation are in good agreement with the spatial distribution of Neogene pediplains described here for the Coastal Cordillera and described in previous works for the eastern Frontal Cordillera (Fig. 9). North of 31°S, the La Silla Pediplain seems to follow the western border of the Main Incaic Range as their remnants are exposed along the western Frontal Cordillera in the area of the Huasco Valley; whereas within the Elqui and Limarí Valleys the La Silla Pediplain is exposed farther to the west forming the highest summits of the eastern Coastal Cordillera (Fig. 5). In the high Frontal Cordillera of the same area (north of 31°S), previous works indicate that Neogene pediplains developed along the eastern Frontal Cordillera, to the east of the position of the Main Incaic Range inferred here (Fig. 9). Thus, Neogene pediplains developed to the west and east of the Main Incaic Relief (Fig. 9). No evidence of Incaic deformation has been described south of 31°S along the Frontal/Principal Cordilleras. However, remnants of the La Silla Pediplain are anyway located immediately to the west of the exposures of Eocene to Oligocene magmatic rocks that mark the position of the Eocene-Oligocene volcanic arc (Fig. 9). Finally, with respect to the pediplains of the western Coastal Cordillera, the differences on exhumation timing to the north and to the south of 30°S are in good agreement with the slight relief display by the Algarrobillo Pediplain north of 30°S and the absence of such relief south of 30°S (Figs 8a, b & 9).

The spatial relationship between the La Silla Pediplain and the areas affected by Eocene–Oligocene uplift and deformation in the Frontal Cordillera suggests a strong control of previous palaeotopography on the Neogene landscape evolution of both the Coastal and Frontal Cordilleras in the study area. Moreover, Neogene pediplains developed to the west and to the east of the position proposed here of the Main Incaic Range (Fig. 9). This is consistent with the previous proposition of Charrier *et al.* (2007), which suggested that the Main Incaic Range may have acted as the Eocene–Oligocene watershed.

Constraints on the original base level and the timing of uplift in the Coastal Cordillera

Low relief/slope surfaces can develop at high elevations (above sea-level) if downstream aggradation occurs, allowing the establishment of a new and higher base level and the concomitant reduction of the erosive efficiency of the drainage system, all of which finally induce the progressive smoothing of the relief upstream (Babault *et al.* 2005).

The geomorphological and geochronological data described above strongly suggest that the La Silla and Algarrobillo Pediplains once formed a single low relief/slope surface. By the Early Miocene this single surface dominated the landscape of the present-day Coastal Cordillera throughout the entire study area (Fig. 11a, b). Importantly, the La Silla–Algarrobillo surface displayed a slight relief north of 30°S, with NNE–NNW-oriented ranges to the west of the Domeyko Depression at relatively higher elevations (Fig. 11a). The presence of a higher topography in this area prior to the Early Miocene is consistent with apatite fission-track and U–Th/He thermochronology (Maksaev *et al.* 2009) indicating that rocks from the western Coastal Cordillera to the west of the Domeyko Depression were exhumed in response to uplift by the Middle–Late Eocene. Moreover, the sedimentology of the Domeyko Gravels also indicates that they accumulated in a closed basin with a local sediment source (Arévalo *et al.* 2009). According to Le Roux *et al.* (2004, 2005, 2006), shallow marine sedimentation related to the Coquimbo Formation was already taking place in the Tongoy Bay and at Punta Choros, immediately to the west of the La Silla–Algarrobillo pediplain by the Early Miocene around *c.* 23 and 18 Ma, respectively (Figs 4 & 9; Coquimbo Formation). This indicates that the original base level for this surface would probably correspond to sea-level at that time. Disruption of the original La Silla–Algarrobillo surface and relative uplift of the eastern Coastal Cordillera with respect to the western Coastal Cordillera occurred after *c.* 17 Ma. It is unclear whether or not the Domeyko Gravels correspond to syntectonic deposits (Garrido 2009). Therefore, more sedimentological and geochronological work is needed to establish if disruption of the original La Silla–Algarrobillo surface occurred between the Early to Middle Miocene or extended into the Middle Miocene. A similar period of uplift in the Early–Middle Miocene is interpreted from apatite fission-track and U–Th/He data that indicate accelerated cooling affecting the central Frontal Cordillera between *c.* 20 and 15 Ma (Cembrano *et al.* 2003; Rodríguez *et al.* 2012). Moreover, Early–Middle Miocene contractional deformation and related uplift would have extended into the eastern Frontal Cordillera according to structural (Winocur 2010; Winocur *et al.* 2014) and geomorphological data (Bissig *et al.* 2002).

After disruption of the original Algarrobillo–La Silla surface, the development at high elevation of the degradational part of the Corredores Pediplain is explained by the geomorphological connection with the top of the Domeyko Gravels. However, the Corredores Pediplain is not geomorphologically continuous with any aggradational surface south of 30°S. One possibility is that in this area the Corredores Pediplain was tectonically uplifted to its present-day elevation by the same north–south faults which previously displaced the La Silla Pediplain (Fig. 9). Nevertheless, south of 30°S the Corredores Pediplain usually presents the same range of elevations (2000–1200 m a.s.l.) as in the Domeyko Depression and it is also always entrenched within the La Silla Pediplain. Therefore, the most probable explanation is that the Corredores Pediplain was actually formed at high elevations due to aggradation to the west of the secondary topographic front throughout the entire study area, but these deposits were later removed south of 30°S. The presence of a topographic barrier to the west of the Domeyko Depression north of 30°S (Figs 8a & 11a) would allow preservation of the Domeyko Gravels after incision of the Corredores Pediplain. In contrast, the absence of such a barrier south of 30°S (Figs 8b & 11b) probably allowed erosion and remobilization of deposits associated with the Corredores Pediplain overlying the Algarrobillo Pediplain. South of 30°S the western border of the Corredores Pediplain coincides with the maximum extension to the east of the Miocene–Pleistocene fluvial facies of the Confluencia Formation (Figs 8b & 9; Emparán & Pineda 2000). These deposits may correspond to the aggradational deposits related to the Corredores Pediplain, later remobilized from the top of the Algarrobillo Pediplain due to incision, and redeposited within the river valleys that incised this surface (Figs 8b & 11b). With respect to the Algarrobillo Pediplain, it is known that marine deposition of the Coquimbo Formation was still taking place to the west by the Late Miocene when incision on top of this pediplain started, as suggested by supergene alunite ages (Figs 5 & 8a; Creixell *et al.* 2012). Since sea-level was the base level for the Algarrobillo Pediplain during most of the Miocene, this surface was necessarily uplifted to its present-day high elevations. Therefore, the incision ages between 7 and 5 Ma indicate that uplift of the Algarrobillo Pediplain started before 7 Ma. Thus, uplift of the Algarrobillo Pediplain probably occurred in the Late Miocene before 7 Ma (Fig. 11a, b). Importantly, the transition between a hyperarid climate to the north of 27°S and a humid climate south of 33°S occurred *c.* 15 Ma (Le Roux 2012). Thus, aggradation of the Middle Miocene Domeyko Gravels and development at high elevations of the degradational part of the Corredores Pediplain may be related, at least in part, to a climatically driven decrease of the transport capacity of rivers (Fig. 11a, b). Most probably, later incision on top of the aggradational/degradational Corredores Pediplain is a consequence of the Late Miocene uplift of the underlying Algarrobillo Pediplain (Fig. 11a, b). Late Miocene uplift of these pediplains is consistent with chronostratigraphic analysis performed in the marine Coquimbo Formation, which has provided evidence of a period of generalized uplift affecting the coastal areas next to the Algarrobillo Pediplain by the Late Miocene (Le Roux *et al.* 2005). Finally, uplift of the Algarrobillo and Corredores Pediplains indicates the present-day western and eastern Coastal Cordilleras were co-evally uplifted by the Late Miocene (Fig. 11a, b).

By the Late Pliocene, the Cachiyuyo Pediplain had developed at the foot of the Algarrobillo and Corredores Pediplains (Fig. 11a, b). The local base level for development of the Cachiyuyo Pediplain is given by the aggradation related to the alluvial and colluvial deposits north of 30°S (Arévalo *et al.* 2009) and the alluvial facies within the Confluencia Formation south of 30°S (Figs 8a, b & 9; Emparán & Pineda 2006). South of 30°S these deposits interfinger towards the centre of the present-day valleys with fluvial facies within the Confluencia Formation (Fig. 8b). Therefore, the base level for the Cachiyuyo Pediplain probably corresponded to the original surface on top of this facies of the Confluencia Formation that was later modified by the pedimentation event leading to formation of the Ovalle Pediplain (Fig. 8b; Rodríguez *et al.* 2013). The Cachiyuyo Pediplain was formed during the Late Pliocene (Table 1). There is no evidence to indicate whether incision of the Cachiyuyo Pediplain has a tectonic or climatic origin. According to geohistorical analysis of the Coquimbo Formation, strong uplift of the coastal area from *c*. 2 Ma has led to the emergence of the Tongoy Bay sediments (Fig. 9; Le Roux *et al.* 2006). Thus, one possibility is that uplift by *c*. 2 Ma would have also affected the Coastal Cordillera to the west of the Tongoy Bay. However, there is no direct evidence pointing to tectonic-related incision of the Cachiyuyo Pediplain (Fig. 11a, b). Finally, according to Rodríguez *et al.* (2013) the Ovalle Pediplain was uplifted *c*. 150 m, after *c*. 500 ka (Fig. 11a, b).

Tectonic versus erosional controls

The similarity in elevation and the latitudinal continuity of the different levels of pediplains described here show that the timing of Neogene surface uplift was similar north and south of the city of La Serena (30°S). Nevertheless, two important differences in pediplain development and preservation are observed between both areas:

(1) North of 30°S the Algarrobillo Pediplain is covered by the Domeyko Gravels (Fig. 8a) that were probably deposited in the Middle Miocene within a basin disconnected from the sea and flanked to the west by NNE ranges. In contrast, south of 30°S the same pediplain is uncovered and more incised according to hypsometric analysis (Aguilar *et al.* 2013). In this area, the Miocene–Pleistocene continental deposits from the Confluencia Formation are encased within the broad valleys that incise the Algarrobillo Pediplain (Fig. 8b). Part of these deposits probably corresponds to material remobilized after the Middle Miocene from an original position on top of the Algarrobillo Pediplain; otherwise the Corredores Pediplain could not have developed at high elevations. Near the coast, the Confluencia Formation changes laterally towards the west into the marine Coquimbo Formation (Fig. 4).

(2) South of 30°S the Ovalle Pediplain is a wide Early–Middle Pleistocene planation surface composed of marine and continental erosion landforms, with the continental erosional surfaces developed on top of the older fluvial gravels of the Confluencia Formation (Fig. 8b). In contrast, to the north of 30°S the Ovalle Pediplain forms a much narrower strip next to the coast that is mainly composed of shore platforms mostly disconnected from continental erosion surfaces inland (Fig. 8a).

In summary, a morphological and sedimentological connection between river and coastal systems is observed south of 30°S which has existed since at least the Early Miocene; however, it is not detected further north. This indicates that the drainage system south of 30°S has presented a larger capacity to incise and transport material towards the sea than the drainage system to the north. According to the sedimentological features of the Domeyko Gravels (Arévalo *et al.* 2009) and the palaeotopography of the Algarrobillo Pediplain, by the Early Miocene the ability of rivers to incise and transport was inhibited by the blocking of the drainage exerted by high NNE-trending ranges just to the west of the Domeyko Depression.

Presently, in spite of the lower elevation of north–south-oriented ranges in the western Coastal Cordillera south of 30°S relative to the NNE–NNW-oriented ranges to the north, low-slope, depressed areas aligned with the Domeyko Depression are also locally observed within the Algarrobillo Pediplain south of La Serena (Fig. 2c). In Figure 2c it is also shown how rivers draining these depressions are captured by higher-order channels within the Elqui and Limarí Valleys. Therefore, the differences in pediplain development after the Early Miocene in both areas seem to be related to the ability of the main channels to capture lower-order channels (Farías 2007). There are three possible explanations for this: (1) the rocks are easier to erode south of 30°S (Farías 2007), (2) the slope is higher south of 30°S (Carretier *et al.* 2013) or (3) the water flow is higher than further north (Whipple & Tucker 1999). The first possibility is ruled out because depressions of both areas are developed on top of the same lithological units, Early Cretaceous granitoids to the west and Lower to Upper Cretaceous volcano-sedimentary rocks to the east. The second possibility is rejected because the regional slope would depend on previous topography (before the Early Miocene) being dominated by the Main Incaic Range that, according to palaeomagnetic data, diminishes in importance south of 31°S. The last possibility is the favoured explanation because water flow depends on the drainage area and precipitation. Indeed, the areas drained by the Elqui, Limarí and Choapa Rivers are evidently higher than the area drained by the rivers in the Domeyko Depression (Fig. 2c). However, the high order of the main channel of the Huasco Valley indicates that its drainage area is also significant and similar to the areas drained by the Elqui, Limarí and Choapa Rivers. This suggests that drainage area could be an important, but not dominant, factor controlling landscape evolution in the study area. However, it is observed that precipitation rises from <100 mm a^{-1} to >200–300 mm a^{-1} south of 30°S (Fig. 2a). This latitude marks the northernmost penetration of the southern hemisphere westerlies, which bring moisture from southern latitudes, opposite to the effect of the Southeast Pacific Anticyclone, the main factor responsible for the hyperaridity of the Atacama Desert to the north. The latitudinal precipitation gradient was acquired after the Middle Miocene by a combination of a series of events including glaciations in West Antartica, formation of the Humboldt Current and uplift of the Andes (Le Roux 2012). Thus, it is proposed here that a rise in water flow due to higher precipitation south of 30°S would have played an important role in determining the differences in geomorphological evolution observed north and south of 30°S since the Middle Miocene. Such a precipitation gradient could have been superimposed on the previous palaeotopography that presented an inherited Incaic component along the Coastal Cordillera, north of 30°S, and along the Frontal Cordillera, north of 31°S. Thus, the palaeotopography inherited from the Eocene–Oligocene (Incaic) phase of uplift and deformation would correspond to a dominant factor controlling Neogene landscape development in the study area.

Uplift timing throughout the study area closely correlates with episodes of increased deformation recognized throughout the western flank of the Andes to the north of 27°S and to the south of 33°S. The Early (Middle?) Miocene uplift stage of the eastern Frontal Cordillera correlates with a period of intense deformation along the western border of the Altiplano of northern Chile (Pinto *et al.* 2004; Victor *et al.* 2004; Farías *et al.* 2005) that is also recognized in southern Perú (Megard 1984) and with the tectonic inversion of the extensional volcano-sedimentary Abanico Basin in central Chile south of 32°S (Charrier *et al.* 2002). The Late Miocene uplift stage of the western and eastern Coastal Cordilleras correlates with regional uplift of the forearc region recognized in southern Perú (Tosdal *et al.* 1984; Clark *et al.* 1990; Quang *et al.* 2005; Schildgen *et al.* 2007), northern Chile (Hoke *et al.* 2007), the Southern Atacama Desert (Riquelme *et al.* 2007) and central Chile south of 33°S (Farías *et al.* 2008*a*, *b*; Maksaev *et al.* 2009). The post-500 ka uplift of the Ovalle Pediplain correlates with a renewal of uplift of marine landforms along the Pacific coast post 400 ± 100 ka after an Early–Middle Pleistocene period of relatively slow uplift identified to the north of La Serena (30°S) by Regard *et al.* (2010). Uplift of the Ovalle Pediplain also correlates with Pleistocene–Holocene uplift of pediments and other continental landforms along the forearc of southern Peru and northern Chile (González *et al.* 2003, 2006; Kober *et al.* 2007; Hall *et al.* 2008; Saillard *et al.* 2009; Jordan *et al.* 2010).

Increased deformation by the Early (Middle?) Miocene would be explained by a more intense stress transmission and widespread strain due to an increased plate convergence rate (Charrier *et al.* 2009, 2013) after break-up of the Farallon Plate into the Nazca and Cocos Plates (Pardo-Casas & Molnar 1987; Somoza 1998). The driving forces for Late Miocene and Middle Pleistocene uplifts are still unclear and a matter of great debate in the case of the Late Miocene (Garzione *et al.* 2006; Barnes & Ehlers 2009), but determining these driving forces is beyond the scope of the study. However, the fact that Late Miocene and Middle Pleistocene uplifts are recognized for such a vast area from southern Perú to central Chile suggests that they were controlled by first-order tectonic features.

Conclusions

Prior to *c.* 17 Ma an extensive pediplain sloping down to sea-level dominated the landscape west of an inherited Main Incaic Range mainly exposed in the present-day Frontal Cordillera (Fig. 11a, b). North of 30°S, this pediplain extended across the entire present-day Coastal Cordillera and was not completely sub-planar as it already presented a slight inherited relief flanking the Domeyko Depression to the west (Fig. 11a). In contrast, south of 30°S the pediplain extended across the present-day Coastal Cordillera, progressively diminishing in elevation towards the sea (Fig. 11b).

In the Early (Middle?) Miocene the pediplain was offset by a series of north–south-trending faults (Fig. 11a, b). The eastern Coastal Cordillera was uplifted with respect to the western Coastal Cordillera throughout the entire study area (Fig. 11a, b). Importantly, offset of the original pediplain is co-eval with a significant period of uplift and exhumation in the Frontal Cordillera to the east. Uplift led to the formation of a secondary topographic front within the present-day Coastal Cordillera and concomitant deposition next to the scarp. Aggradation to the west of the scarp and development of degradational pediplains at high elevations by the Late Miocene (Fig. 11a, b) may have been favoured by the establishment of the observed latitudinal precipitation gradient throughout the study region after the Middle Miocene (Le Roux 2012). North of 30°S the aggradational deposits accumulated within the Domeyko Depression (Fig. 11a). In contrast, south of 30°S the absence of a topographic barrier to the west and probable higher precipitation rate compared to the north prevented preservation of the aggradational deposits, which were later remobilized (Fig. 11b).

By the Late Miocene, the entire Coastal Cordillera was uplifted (Fig. 11a, b). South of 30°S, uplift generated a rejuvenation of the drainage system, generating material that had previously accumulated to the west of the secondary topographic front and which was remobilized and redeposited by fluvial systems similar to those of the present-day (Fig. 11b). Between the Early and Middle Pleistocene a new pediplain, partly carved on top of these deposits and connected with shore platforms towards the coast, developed southwards from La Serena, whereas to the north only the shore platforms developed (Fig. 11b). Finally, this pediplain was uplifted post-500 ka.

The uplift stages recognized for the study area correlate with episodes of increased deformation widely recognized throughout the western flank of the Andes both to the north and to the south of the study area. Uplift by the Early (-Middle?) Miocene correlates with the Late Oligocene–Early Miocene episode of increase plate convergence between the Nazca and South American Plates, but the driving forces for Late Miocene and Middle Pleistocene uplift remain unclear. The differences in landscape development recognized between the regions located to the north and south of 30°S, respectively, are probably related to differences in the previous palaeotopography along the western Frontal Cordillera and the first-order climatic transition at 30°S that defines the southernmost reaches of the Atacama Desert.

This study was supported in part by the Chilean Government through the Comisión Nacional de Ciencia y Tecnología CONICYT (Anillo ACT-18 project, AMTC), the Advanced Mining Technology Center (AMTC) of the Facultad de Ciencias Físicas y Matemáticas, Universidad de Chile; FONDECYT Project 11085022 'Interacción Clima-Tectónica en el Alzamiento Andino de Chile Central durante el Neógeno'; FONDECYT N° 11121529, FONDECYT N° 1120272, the Ecos-Conicyt proyect C11U02 'Levantamiento de la costa pacífica de Sud América y acoplamiento interplaca en la zona de subducción'. Additional support was obtained by IRD Project 'Erosión en los Andes'.

This study is part of the PhD theses of M.P. Rodríguez and G. Aguilar, both of whom were supported by 4-year grants from CONICYT, the Universidad Católica del Norte and Égide-France (Bourse d'excellence Eiffel). Useful discussions with S. Carretier, M. Farías and V. Tolorza helped develop and clarify our ideas. The authors would like to express their thanks for the constructive comments by two anonymous reviewers which led to significant improvements in the manuscript.

References

Aguilar, G., Riquelme, R., Martinod, J., Darrozes, J. & Maire, E. 2011. Variability in erosion rates related to the state of landscape transience in the semi-arid Chilean Andes. *Earth Surface Processes and Landforms,* **36**, 1736–1748, http://dx.doi.org/10.1002/esp.2194

Aguilar, G., Riquelme, R., Martinod, J. & Darrozes, J. 2013. Role of climate and tectonics in the geomorphologic evolution of the Semiarid Chilean Andes between 27–32°S. *Andean Geology* **40**, 79–101, http://dx.doi.org/10.5027/andgeoV40n1-a04

Arancibia, G. 2004. Mid-Cretaceous crustal shortening: evidence from a regional-scale ductile shear zone in the Coastal Range of central Chile (328 S). *Journal of South American Earth Sciences*, **17**, 209–226.

Arancibia, G., Matthews, S. J. & Pérez de Arce, C. 2006. K-Ar and $^{40}Ar/^{39}Ar$ geochronology of supergene processes in the Atacama Desert, Northern Chile: tectonic and climatic relations. *Journal of the Geological Society*, **163**, 107–118, http://dx.doi.org/10.1144/0016-764904-161.

Arévalo, C., Mourgues, F. A. & Chávez, R. 2009. *Geología del Área Vallenar-Domeyko, Región de Atacama*. Servicio Nacional de Geología y Minería, Carta Geológica de Chile.

Arriagada, C., Mpodozis, C., Yañez, G., Roperch, P., Charrier, R. & Farías, M. 2009. Rotaciones Tectónicas en Chile Central: El Oroclino de Vallenar y el 'Megakink' del Maipo. *XII Congreso Geológico Chileno*, Santiago, Chile, 23–26 November, Departamento de Geología de la Universidad de Chile.

Arriagada, C., Ferrando, R., Córdova, L., Morata, D. & Roperch, P. 2013. The Maipo Orocline: a first scale structural feature in the Miocene to Recent geodynamic evolution in the central Chilean Andes. *Andean Geology*, **40**, 419–437, http://dx.doi.org/10.5027/andgeoV40n3-a02.

Babault, J., Van Den Driessche, J., Bonnet, S., Castelltort, S. & Crave, A. 2005. Origin of the highly elevated Pyrenean peneplain. *Tectonics*, **24**, TC2010, http://dx.doi.org/10.1029/2004TC001697

Barnes, J. B. & Ehlers, T. A. 2009. End member models for Andean Plateau uplift. *Earth Science Review* **97**, 105–132.

Benado, D. E. 2000. *Estructuras y estratigrafía básica de terrazas marinas en sector costero de Altos de Talinay y Bahía Tongoy, implicancias neotectónicas*. Msc Thesis, Departamento de Geología, Universidad de Chile, Santiago.

Bissig, T. 2001. *Metallogenesis of the Miocene El Indio-Pascua gold-silver-copper belt, Chile/Argentina: Geodynamic, Geomorphological and Petrochemical controls on epithermal mineralization*. PhD thesis, Queen's University.

Bissig, T. & Riquelme, R. 2010. Andean uplift and climate evolution in the southern Atacama Desert deduced from geomorphology and supergene alunite-group minerals. *Earth and Planetary Science Letters*, **299**, 447–457.

Bissig, T., Lee, J. K. W., Clark, A. H. & Heather, K. B. 2001. The Cenozoic History of volcanism and hydrothermal alteration in the Central Andes Flat-Slab Region: New ^{40}Ar-^{39}Ar constraints from the El Indio-Pascua Au (-Ag, Cu) Belt, 29°20′–30°30′S. *International Geology Review*, **43**, 1–29.

Bissig, T., Clark, A. H., Lee, J. K. W. & Hodgson, C. J. 2002. Miocene landscape evolution and geomorphologic controls on epithermal processes in the El Indio-Pascua Au–Ag–Cu belt, Chile and Argentina. *Economic Geology and the Bulletin of the Society of Economic Geologists*, **97**, 971–996, http://dx.doi.org/10.2113/97.5.971

Bissig, T., Clark, A. H., Lee, J. K. W. & von Quadt, A. 2003. Petrogenetic and Metallogenetic responses to Miocene slab flattening: new constraints from the El Indio-Pascua Au-Ag-Cu belt, Chile/Argentina. *Mineralium Deposita*, **38**, 844–862.

Cahill, T. & Isacks, B. L. 1992. Seismicity and shape of the subducted Nazca plate. *Journal of Geophysical Research*, **97**, 17503–17529.

Cancino, G. 2007. *Hoja El Transito mapa de compilación, 1:250 000*, SERNAGEOMIN.

Carretier, S., Regard, V. *et al.* 2013. Slope and climate variability control of erosion in the Andes of central Chile. *Geology*, **41**, 195–198, http://dx.doi.org/10.1130/G33735.1

Cembrano, J., Zentilli, M., Grist, A. & Yañez, G. 2003. Nuevas edades de trazas de fisión para Chile Central (30°–34°S): Implicancias en el alzamiento y exhumación de los Andes desde el Cretácico. *10° Congreso Geológico Chileno*, Concepción, Chile, 6–10 October, Departamento de Ciencias de la Tierra, Universidad de Concepción.

Charrier, R. & Vicente, J. C. 1972. Liminary and geosynclinal Andes: major orogenic phases and synchronical evolution of the central and Magellan sectors of the Argentine-Chillean Andes. *In*: *International Upper Mantle Project Conference on Solid Earth Problems, Proceedings, 26–31 October, Buenos Aires*, Comité Argentino del Manto Superior, **2**, 451–470.

Charrier, R., Baeza, O. *et al.* 2002. Evidence for Cenozoic extensional basin development and tectonic inversion south of the flat-slab segment, southern Central Andes, Chile (33°–36°S.L.). *Journal of South American Earth Sciences*, **15**, 117–139.

Charrier, R., Pinto, L. & Rodríguez, M. P. 2007. Tectonostratigraphic evolution of the Andean Orogen in Chile. *In*: Moreno, T. & Gibbons, W. (eds) *The Geology of Chile*. The Geological Society, London, 21–114.

Charrier, R., Farias, M. & Maksaev, V. 2009. Evolución tectónica, paleogeográfica y metalogénica durante el Cenozoico en los Andes de Chile norte y central e implicaciones para las regiones adyacentes de Bolivia y Argentina. *Revista de la Asociación Geológica Argentina*, **65**, 5–35.

Charrier, R., Herail, G., Pinto, L., Garcia, M., Riquelme, R., Farias, M. & Muñoz, N. 2013. Cenozoic tectonic evolution in the Central Andes in northern Chile and west central Bolivia: implications for paleogeographic, magmatic and mountain building evolution. *International Journal of Earth Sciences*, **102**, 235–264.

Clark, A. H., Tosdal, R. M., Farrar, E. & Plazolles, A. 1990. Geomorphologic environment and age of supergene enrichment of the Cuajone, Quellaveco, and Toquepala Porphyry Copper-Deposits, Southeastern Peru. *Economic Geology and the Bulletin of the Society of Economic Geologists*, **85**, 1604–1628.

Clark, M. K., Royden, L. H., Whipple, K. X., Burchfiel, B. C., Zhang, X. & Tang, W. 2006. Use of a regional, relict landscape to measure vertical deformation of the eastern Tibetan Plateau. *Journal of Geophysical Research*, **111**, F03002, http://dx.doi.org/10.1029/2005JF000294

Cooke, R., Warren, A. & Goudie, A. 1993. *Desert Geomorphology*. UCL Press, London.

Cornejo, P., Mpodozis, C., Ramírez, C. F. & Tomlinson, A. J. 1993. *Estudio geológico de la Región de Potrerillos y El Salvador (26°–27° Latitude S)*. Servicio Nacional de Geología y Minería - Corporación del Cobre, Informe Registrado, IR-93-01, Volume **1**, Santiago.

Cornejo, R., Matthews, S. & Pérez de Arce, C. 2003. The 'K-T' compressive deformation event in northern Chile (24–27°S). *In*: *10° Congreso Geológico Chileno*, Concepción, Chile, 6–10 October, Departamento de Ciencias de la Tierra, Universidad de Concepción.

Creixell, C., Ortiz, M. & Arévalo, C. 2012. *Geología del área Carrizalillo-El Tofo, Región de Atacama, Servicio Nacional de Geología y Minería, 1 mapa escala 1:100 000*. Carta Geológica de Chile, Serie Geología Básica.

Emparán, C. & Calderón, M. 2008. *Geología del area Ovalle-Peña Blanca, Región de Coquimbo*. Servicio Nacional de Geología y Minería, Santiago.

Emparán, C. & Pineda, G. 2000. *Geología del area La Serena-Higuerillas, Región de Coquimbo*. Servicio Nacional de Geología y Minería, Santiago.

Emparán, C. & Pineda, G. 2006. *Geología del Area Andacollo-Puerto Aldea, Región de Coquimbo*. Carta Geológica de Chile, Serie Geológica Básica.

Farías, M. 2007. *Tectónica y erosión en la evolución del relieve de los Andes de Chile Central durante el Neógeno*. *PhD thesis*, Universidad de Chile y Université de Toulouse III, (inédito), Santiago–Toulouse.

Farías, M., Charrier, R., Comte, D., Martinod, J. & Herail, G. 2005. Late Cenozoic deformation and uplift of the western flank of the Altiplano: evidence from the depositional, tectonic, and geomorphologic evolution and shallow seismic activity (northern Chile at 19 degrees 30°S). *Tectonics*, **24**, TC4001, http://dx.doi.org/10.1029/2004TC001667

Farías, M., Charrier, R. *et al.* 2008*a*. Late Miocene high and rapid surface uplift and its erosional response in the Andes of central Chile (33°–35°S). *Tectonics*, **27**, Tc1005, http://dx.doi.org/10.1029/2006tc002046

Farías, M., Charrier, R. *et al.* 2008*b*. No subsidence in the development of the Central Depression along the Chilean margin. *7th Symposium on Andean Geodynamics*, Nice, France, 2–4 September, 206–209, Institute de recherche pour le développement (IRD).

García, M. & Hérail, G. 2005. Fault-related folding, drainage network evolution and valley incision during the Neogene in the Andean Precordillera of Northern Chile. *Geomorphology*, **65**, 279–300.

Garrido, G. 2009. *Evolución geomorfológica de la Depresión de Domeyko entre los 28°45′–29°00′S durante el Neógeno*. *Thesis*, Departamento de Geología, Universidad de Chile.

Garzione, C. N., Molnar, P., Libarkin, J. C. & MacFadden, B. 2006. Rapid late Miocene rise of the Andean plateau: evidence for removal of mantle lithosphere. *Earth and Planetary Science Letters*, **241**, 543–556.

Giambiagi, L., Mescua, J., Bechis, F., Tassara, A. & Hoke, G. 2012. Thrust belts of the southern Central Andes: along-strike variations in shortening, topography, crustal geometry, and denudation. *Geological Society of America Bulletin*, **124**, 1339–1351, http://dx.doi.org/10.1130/B30609.1

González, G., Cembrano, J., Carrizo, D., Macci, A. & Schneider, H. 2003. Link between forearc tectonics and Pliocene-Quaternary deformation of the Coastal Cordillera, Northern Chile. *Journal of South American Earth Sciences*, **16**, 321–342.

González, G., Dunai, T., Carrizo, D. & Allmendinger, R. 2006. Young displacements on the Atacama Fault System, northern Chile from field observations and cosmogenic ^{21}Ne concentrations. *Tectonics*, **25**, TC3006, http://dx.doi.org/10.1029/2005TC001846.

Hall, S. R., Farber, D. L., Audin, L., Finkel, R. C. & Mériaux, A.-S. 2008. Geochronology of pediment surfaces in southern Peru: implications for Quaternary deformation of the Andean forearc. *Tectonophysics*, **459**, 186–205.

Hilley, G. E. & Coutand, I. 2010. Links between topography, erosion, rheological heterogeneity, and deformation in contractional settings: insights from the Central Andes. *Tectonophysics*, **95**, 78–92.

Hilley, G. E., Strecker, M. R. & Ramos, V. A. 2004. Growth and erosion of fold-and-thrust belts, with an application to the Aconcagua Fold-and-Thrust Belt, Argentina. *Journal of Geophysical Research, Solid Earth*, **109**, B01410, http://dx.doi.org/10.1029/2002JB 002282.

Hoke, G. D., Isacks, B. L., Jordan, T. E., Blanco, N., Tomlinson, A. J. & Ramezani, J. 2007. Geomorphic evidence for post-10 Ma uplift of the western flank of the central Andes 18°30′–22°S. *Tectonics*, **26**, TC5021, http://dx.doi.org/10.1029/2006TC002082.

Isacks, B. 1988. Uplift of the central Andean plateau and bending of the Bolivian orocline. *Journal of Geophysical Research: Solid Earth*, **93**, 3211–3231.

Jara, P. & Charrier, R. 2014. Nuevos antecedentes estratigráficos y geocronológicos para el Meso-Cenozoico de la Cordillera Principal de Chile entre 32° y 32°30'S: Implicancias estructurales y paleogeográficas. *Andean Geology*, **41**, 174–209, http://dx.doi.org/10.5027/andgeoV41n1-a07.

Jordan, T. E., Isacks, B. L., Allmendinger, R. W., Brewer, J. A., Ramos, V. A. & Ando, C. J. 1983. Andean tectonics related to geometry of subducted Nazca plate. *Geological Society of America Bulletin*, **94**, 341–361.

Jordan, T. E., Nester, P. L., Blanco, N., Hoke, G. D., Dávila, F. & Tomlinson, A. J. 2010. Uplift of the Altiplano-Puna plateau: a view from the west. *Tectonics*, **29**, TC5007, http://dx.doi.org/10.1029/2010TC002661

Kay, S. & Mpodozis, C. 2002. Magmatism as a probe to the Neogene shallowing of the Nazca plate beneath the modern Chilean flatslab. *Journal of South American Earth Science*, **15**, 39–59.

Kober, F., Ivy-Ochs, S., Schlunegger, F., Baur, H., Kubik, P. W. & Wieler, R. 2007. Denudation rates and a topography-driven rainfall threshold in northern Chile: Multiple cosmogenic nuclide data and sediment yield budgets. *Geomorphology*, **83**, 97–120.

Lamb, S. & Davis, P. 2003. Cenozoic climate change as a possible cause for the rise of the Andes. *Nature*, **425**, 792–797, http://dx.doi.org/10.1038/nature02049

Lamb, S., Hoke, L., Kennan, L. & Dewey, J. 1997. Cenozoic evolution of the Central Andes in Bolivia and northern Chile. *In*: Burg, J. -P. & Ford, M. (eds) *Orogeny Through Time*. Geological Society, London, Special Publications, **121,** 237–264.

Le Roux, J. P. 2012. A review of Tertiary climate changes in southern South America and the Antarctic Peninsula. Part 2: continental conditions. *Sedimentary Geology*, **247**, 21–38.

Le Roux, J. P., Gómez, C., Fenner, J. & Middleton, H. 2004. Sedimentological processes in a scarp-controlled rocky shoreline to upper continental slope environment, as revealed by unusual sedimentary features in the Neogene Coquimbo Formation, north-central Chile. *Sedimentary Geology*, **165**, 67–92.

Le Roux, J. P., Gómez, C. et al. 2005. Neogene–Quaternary coastal and offshore sedimentation in north-central Chile: record of sea level changes and implications for Andean tectonism. *Journal of South American Earth Sciences*, **19**, 83–98.

Le Roux, J. P., Olivares, D. M., Nielsen, S. N., Smith, N. D., Middleton, H., Fenner, J. & Ishman, S. E. 2006. Bay sedimentation as controlled by regional crustal behaviour, local tectonics and eustatic sea-level changes: Coquimbo Formation (Miocene–Pliocene), Bay of Tongoy, central Chile. *Sedimentary Geology*, **184**, 133–153.

Ludwig, K. R. 2009. *SQUID 2 (rev*. 2.50), A user's manual, Berkeley Geochronology Center. Special Publications, **5**.

Maksaev, V. & Zentilli, M. 1999. Fission track thermochronology of the Domeyko Cordillera, northern Chile: implications for Andean tectonics and porphyry copper metallogenesis. *Exploration and Mining Geology*, **8**, 65–89.

Maksaev, V., Moscoso, R., Mpodozis, C. & Nasi, C. 1984. Las unidades volcánicas y plutónicas del Cenozoico superior entre la Alta Cordillera del Norte Chico (29°–31°S), geología, alteración hidrotermal y mineralización. *Revista Geológica de Chile*, **21**, 11–51.

Maksaev, V., Munizaga, F., Zentilli, M. & Charrier, R. 2009. Fission track thermochronology of Neogene plutons in the Principal Andean Cordillera of central Chile (33–35°S). Implications for Tectonic Evolution and Porphyry Cu-Mo Mineralization. *Andean Geology*, **36**, 153–171.

Martin, M. W., Kato, T. T., Rodriguez, C., Godoy, E., Duhart, P., McDonough, M. & Campos, A. 1999. Evolution of the late Paleozoic accretionary complex and overlying forearc-magmatic arc, south central Chile (38°–41°S): constraints for the tectonic setting along the southwestern margin of Gondwana. *Tectonics*, **18**, http://dx.doi.org/10.1029/1999TC900021

Megard, F. 1984. The andean orogenic period and its major structures in Central and Northern Peru. *Journal of the Geological Society*, **141**, 893–900.

Mortimer, C. 1973. The Cenozoic history of the southern Atacama Desert, Chile. *Journal of the Geological Society, London*, **129**, 505–526, http://dx.doi.org/10.1144/gsjgs.129.5.0505

Moscoso, R., Nasi, C. & Salinas, P. 1982. *Hoja Vallenar y parte norte de La Serena, geological map, 1:250 000*. SERNAGEOMIN.

Mpodozis, C. & Cornejo, P. 1988. *Hoja Pisco Elqui. IV Región de Coquimbo*. Servicio Nacional de Geología y Minería, Carta Geológica de Chile, No. 68, Santiago.

Mpodozis, C., Brockway, H., Marquardt, C. & Perelló, J. 2009. Geocronología U/Pb y tectónica de la región de Los Pelambres-Cerro Mercedario: implicancias para la evolución cenozoica de Los Andes del centro de Chile y Argentina. *In*: *XII Congreso Geológico Chileno*, **12**, Santiago, Chile, 23–26 November, Departamento de Geología de la Universidad de Chile.

Nalpas, T., Dabard, M.-P., Pinto, L. & Loi, A. 2009. Preservation of the Miocene Atacama Gravels in Vallenar area, northern Chilean Andes: climate, stratigraphic or tectonic control? *XII Congreso Geológico Chileno*, Santiago, 23–26 November, Departamento de Geología de la Universidad de Chile.

Nasi, C., Moscoso, R. & Maksaev, V. 1990. *Hoja Guanta, Regiones de Atacama y Coquimbo*, Sernageomin, Santiago, Chile.

Ota, Y., Miyauchi, T., Paskoff, R. & Koba, M. 1995. Plio–Quaternary terraces and their deformation along the Altos de Talinay, North–Central Chile. *Revista Geologica de Chile*, **22**, 89–102.

Pardo-Casas, F. & Molnar, P. 1987. Relative motion of the Nazca (Farallón) and South American plates since Late Cretaceous time. *Tectonics*, **6**, 233–248.

Paskoff, R. 1970. *Recherches géomorphologiques dans le Chili semi-aride*. Biscaye Freres, Bordeaux.

Pineda, G. & Calderón, M. 2008. *Geología del área Monte Patria-El Maqui, región de Coquimbo, Escala 1:100 000*. Carta Geológica de Chile, Serie Geología Básica, n.116, SERNAGEOMIN: 44 h. Santiago.

Pineda, G. & Emparán, C. 2006. *Geología del area Vicuña-Pichasca, Región de Coquimbo*. Servicio Nacional de Geología y Minería, Santiago.

Pinto, L., Hérail, G. & Charrier, R. 2004. Sedimentación sintectónica asociada a las estructuras neógenas en el borde occidental del plateau andino en la zona de Moquella (19°15′S, Norte de Chile). *Revista Geológica de Chile*, **31**, 19–44.

Quang, C. X., Clark, A. H., Lee, J. K. W. & Hawkes, N. 2005. Response of supergene processes to episodic Cenozoic uplift, pediment erosion, and ignimbrite eruption in the porphyry copper province of southern Peru. *Economic Geology*, **100**, 87–114, http://dx.doi.org/10.2113/100.1.0087

Ramos, V., Cegarra, M. & Cristallini, E. 1996. Cenozoic tectonics of the High Andes of west-central Argentina (30–36°S latitude). *Tectonophysics*, **259**, 185–200.

Ramos, V., Zapata, T., Cristallini, E. & Intracaso, A. 2004. The Andean thrust system-latitudinal variations in structural styles and orogenic shortening. *In*: McClay, K. R. (ed.) *Thrust Tectonics and Hydrocarbon Systems*. AAPG Memoir, **82**, 30–50.

Regard, V., Saillard, M. *et al.* 2010. Renewed uplift of the Central Andes Forearc revealed by coastal evolution during the Quaternary. *Earth and Planetary Science Letters*, **297**, 199–210.

Riquelme, R., Martinod, J., Hérail, G., Darrozes, J. & Charrier, R. 2003. A geomorphological approach to determining the Neogene to Recent tectonic deformation in the Coastal Cordillera of northern Chile (Atacama). *Tectonophysics*, **361**, 255–275.

Riquelme, R., Hérail, G., Martinod, J., Charrier, R. & Darrozes, J. 2007. Late Cenozoic geomorphologic signal of Andean forearc deformation and tilting associated with the uplift and climate changes of the Southern Atacama Desert (26°S–28°S). *Geomorphology*, **86**, 283–306, http://dx.doi.org/10.1016/j.geomorph.2006.09.004

Rivano, S. & Sepúlveda, P. 1991. *Hoja Illapel, Región de Coquimbo*. Carta Geológica de Chile, Sernageomin, Santiago, Chile.

Rodríguez, M. P., Charrier, R., Carretier, S., Brichau, S. & Farías, M. 2012. Alzamiento y exhumación Cenozoicos en el Norte Chico de Chile (30 a 33°S). *XIII Congreso Geológico Chileno*, Antofagasta, Chile, 5–9 August.

Rodríguez, M. P., Carretier, S. *et al.* 2013. Geochronology of pediments and marine terraces in north-central Chile and their implications for Quaternary uplift in the Western Andes. *Geomorphology*, **180–181**, 33–46.

Saillard, M., Hall, S. R. *et al.* 2009. Non-steady long-term uplift rates and Pleistocene marine terrace development along the Andean margin of Chile (31°S) inferred from 10Be dating. *Earth and Planetary Science Letters*, **277**, 50–63.

Salazar, E. 2012. *Evolución tectonica-estratigrafica post-Paleozoica de la Cordillera de Vallenar. Thesis*, Departamento de Geología, Universidad de Chile.

Schildgen, T. F., Hodges, K. V., Whipple, K. X., Reiners, P. W. & Pringle, M. S. 2007. Uplift of the western margin of the Andean plateau revealed from canyon incision history, southern Peru. *Geology*, **35**, 523–526.

SERNAGEOMIN 2003. Carta Geológica de Chile (escala 1:1 000 000) Servicio Nacional de Geología y Minería.

Sillitoe, R. H., Mortimer, C. & Clark, A. H. 1968. A chronology of landform evolution and supergene mineral alteration, Southern Atacama Desert, Chile. *Institute of Mining and Metallurgy Transactions (Section B)*, **27**, 166–169.

Sobel, E. R. & Strecker, M. R. 2003. Uplift, exhumation, and precipitation: tectonics and climatic control of Late Cenozoic landscape evolution in the northern Sierras Pampeanas, Argentina. *Basin Research*, **15**, 431–451.

Somoza, R. 1998. Updated Nazca (Farallon)-South America relative motions during the last 40 My: implications for mountain building in the central Andean region. *Journal of South American Earth Sciences*, **11**, 211–215.

Steinmann, G. 1929. *Geologie von Peru*. Kart Winter, Heidelberg.

Strecker, M. R., Alonso, R. N., Bookhagen, B., Carrapa, B., Hilley, G. E., Sobel, E. R. & Trauth, M. H. 2007. Tectonics and climate of the southern central Andes. *Annual Review of Earth and Planetary Sciences*, **35**, 747–787, http://dx.doi.org/10.1146/annurev.earth.35.031306.140158

Tassara, A. & Yañez, G. 2003. Relación entre el espesor elástico de la litosfera y la segmentación tectónica del margen andino (15–47°S). *Revista Geológica de Chile*, **30**, 159–186.

Tosdal, R. M., Clark, A. H. & Farrar, E. 1984. Cenozoic polyphase landscape and tectonic evolution of the Cordillera Occidental, Southernmost Peru. *Geological Society of America Bulletin*, **95**, 1318–1332.

Urresty, C. 2009. *Evolución geomorfológica de la parte sur de la Depresión de Domeyko (29°00′–29°40′S) durante el Neógeno. Thesis*, Departamento de Geología, Universidad de Chile.

Veit, H. 1996. Southern westerlies during the Holocene deduced from geomorphological and pedological studies in the Norte Chico, northern Chile (27–33°S). *Palaeogeography, Palaeoclimatology, Palaeoecology*, **123**, 107–119.

Victor, P., Oncken, O. & Glodny, J. 2004. Uplift of the western Altiplano plateau (Northern Chile). *Tectonics*, **23**, TC4004, http://dx.doi.org/101029/2003TC001519

Villagrán, C., Leon, A. & Roig, F. A. 2004. Paleodistribution of the alerce and cypres of the Guaitecas during the interstadial stages of the Llanquihue glaciation: Llanquihue and Chiloe provinces, Los Lagos Region, Chile. *Revista Geológica de Chile*, **31**, 133–151.

Whipple, K. X. & Tucker, G. E. 1999. Dynamics of the stream-power river incision model: implications for height limits of mountain ranges, landscape response timescales and research needs. *Journal of Geophysical Research*, **104**, 17661–17674.

Winocur, D. 2010. *Geología y estructura del Valle del Cura y el sector central del Norte Chico, provincia de San Juan y IV Región de Coquimbo, Argentina y Chile. PhD thesis*. Universidad de Buenos Aires, (inédito), Buenos Aires.

Winocur, D. A., Litvak, V. & Ramos, V.2014. Magmatic and tectonic evolution of the Oligocene Valle del Cura basin, Main Andes of Argentina and Chile: evidence for generalized extension. *In*: Sepúlveda, S. A., Giambiagi, L. B., Moreiras, S. M., PINTO, L., Tunik, M., Hoke, G. D. & Farías, M. (eds) *Geodynamic Processes in the Andes of Central Chile and Argentina*. Geological Society, London, Special Publications, **399**. First published online February 17, 2014, http://dx.doi.org/10.1144/SP399.2

Yañez, G. A., Ranero, R. & Huene, V. 2001. Magnetic anomaly interpretation across the southern central Andes (32°–34°S). The role of the Juan Fernández Ridge in the late Tertiary evolution of the margin, *Journal of Geophysical Research–Solid Earth*, **196**, 6325–6345.